Low density lipoprotein receptor-related protein 1 promotes synthetic phenotype of pulmonary artery smooth muscle cells in pulmonary hypertension

Inaugural Dissertation

Submitted to the

Faculty of Medicine

of the Justus Liebig University Giessen

by

Zucker, Marius Michael

from Duisburg, Germany

Giessen 2021

Faculty of Medicine of the Justus Liebig University, Giessen
From the Department of Internal Medicine

Supervisor and Committee Member: Prof. Dr. Wygrecka

Committee Member: PD Dr. Battmann (external reviewer)

Committee Member: Prof. Dr. Bartkuhn (chairman)

Committee Member: Prof. Dr. Reuter

Date of Doctoral Defense: 30.08.2022

Table of contents

1. Introduction

1.1 Definition and etiology of pulmonary hypertension (PH)

Pulmonary Hypertension (PH) is a severe pulmonary disorder originating from multiple causes. PH is defined by a mean pulmonary artery pressure (mPAP) above 25mmHg which leads to an increased right heart hypertrophy with subsequent right heart insufficiency. This disease can progress for a long period of time asymptomatic, mostly starting with exercise dyspnea following by unspecific symptoms such as fatigue, dizziness and syncope (1). In an advanced PH, right ventricular insufficiency leads to additional symptoms like edema and distension of the abdomen (2). Sever PH eventually results in lethal acute right heart failure. Because of a variety of origins, that can result in PH, the World Health Organization classified PH in 5 groups (1). This allows a categorization of pathological similarities, therapeutic approaches and clinical appearance. The group 1 is defined as pulmonary arterial hypertension (PAH), this group compromises all idiopathic, heritable, drug- and infection- induced PH forms. The group 2 is defined as pulmonary venous hypertension, due to left heart insufficiency, that leads to the accumulation of blood in the lung veins and further in the pulmonary arteries. Lung diseases that elevate the mPAP belong to the group 3 of PH. Thrombi, occluding constantly lung arteries leading to an elevated mPAP, is defined as chronic thromboembolic pulmonary hypertension in the group 4. Forms of PH that cannot be assigned to any of these groups are collected in the group 5. These are primarily metabolic or hematologic disorders (1). Except from some entities in the group 1, the manifestation of PH in other groups mostly results from an exacerbation of the underlying disorder, so that treating the underlying disorder may also help tackling PH.

1.2 Epidemiology of pulmonary arterial hypertension (PAH)

The incidence and prevalence are recorded of PAH and other PH forms in Europe by COMPERA (3) (Comparative, Prospective Registry of Newly Initiated Therapies for Pulmonary Hypertension) in the USA by REVEAL (4) (Registry to Evaluate Early and Long-term PAH disease management). In general, PAH is diagnosed by right heart catherization with the advantage of precisely monitoring the patient's parameters, such as mPAP and Wedge pressure (5). However, this intervention needs a clear indication because of its risks, so that there might be many unreported cases. In order to estimate the mPAP non-invasive echocardiography is the method of choice.

The incidence of PAH in Germany is 3.9 cases per million adults, whereas the prevalence is 25.9 cases per million adults (6). Results from the COMPERA registry showed that especially young women are susceptible to develop PAH, however seniors of both sexes are almost equally affected by PAH (3).

1.3 Pathogenesis of PAH

1.3.1 Histological alterations

The pathogenesis of PH is still not fully understood, as it seems to be multifactorial and complex. Despite the different subcategories in PH, the development of this disorder shows similarities throughout the groups. There are pathological alterations in all three layers of the vessels involving endothelium, tunica media and adventitia. Dysfunction and proliferation of endothelial cells as well as plexiform lesion formation are frequently observed phenomena in PH. Plexiform lesions are pathological alterations of the vessels arising from excessive proliferation of endothelial cells. In the tunica media, smooth muscle cell proliferation leads to an exacerbated muscularization of the pulmonary artery but also in the adventitia, fibroblasts increasingly proliferate and produce extracellular matrix proteins. Especially medium- and small-sized arteries, which are under physiological conditions non-muscularized, are affected by this remodeling process (7-9).

1.3.2 Key molecular players involved in the vascular remodeling in PAH

Vascular tone and its regulation are essential in the physiology of the lung in order to provide an ideal oxygen yield for the body. Euler and Liljestrand reported that lung arteries responded to hypoxic conditions with a vasoconstriction in the animal model. Consequently, shifting lung perfusion from less to more ventilated areas optimizes blood oxygenation. This mechanism is primarily conducted by the vasoconstriction of pre-capillary small arteries and is called hypoxic pulmonary vasoconstriction (10,11). In contrast to this mechanism, systemic arteries are responding to hypoxia with vasodilation, in order to cover the oxygen demands of the brain, heart and other organs (12). In general, the pulmonary vascular tone is modified by many factors, ranging from vasodilatory and vasoconstrictive agents and mitochondrial function. A peptide hormone endothelin (ET) attracted much attention in the context of pulmonary vasoconstriction and its relevance in PAH.

1.3.2.1 Endothelin, Prostacyclin and Nitric Oxide

Endothelin was first discovered in 1988 as a powerful vasoconstrictor (13) associated with PAH as its plasma concentration (14) and the level in the muscular layer of pulmonary arteries (15) were found to be elevated in this pathological condition. The endothelium produces the peptide ET, which activates in an autocrine/paracrine manner either ET_A or ET_B-receptors. The distribution of the ET receptors depends on the cell-type in the pulmonary artery: the ET_A-receptor is widely expressed on pulmonary arterial smooth muscle cells (PASMC) (16), while the ET_B -receptor is mostly expressed on the

endothelium of pulmonary arteries. Endothelin can be expressed in three different isoforms, ET-1, ET-2 and ET-3. All ET isoforms bind to the ET_A and ET_B receptor with different affinities. Activation of ET_A-receptor on PASMC leads to contraction of the cells. This effect is mediated by phospholipase C activation and phosphatidylinositol-3 (IP3) production, which leads to the release of Ca^{2+} from endoplasmic reticulum. Moreover, a pro-proliferative cascade, the Ras/Raf pathway, is triggered by the activation of the ET_A-receptor (17). The ET_B-receptor is considered as a part of a negative feedback loop, that is activated in an autocrine manner by the release of ET from the endothelium. The activation of the endothelial ET_B-receptor leads to nitric oxide (NO) production by the endothelium and thus antagonizes ET mediated vasoconstriction (18).

Prostacyclin (PGI2), a vasodilatory agent, is produced by endothelial cells by the PGI2-synthase. PGI2 binds to the prostacyclin receptor that activates an adenylylcyclase, which catalyzes cyclic adenosine monophosphate (cAMP) from ATP. Cyclic adenosine monophosphate decreases intracellular levels of Ca^{2+} in PASMC promoting relaxation of these cells. The expression of the PGI2-synthase is decreased in PAH patients as compared to healthy controls, thus further contributing to the vasoconstriction of pulmonary arteries (19). Nitric oxide production is essential to balance vasoreactivity. It induces a vasorelaxing effect on smooth muscle cells (SMC). Nitric oxide is produced by endothelial cells exposed to shear stress, ET or bradykinin. Nitric oxide diffuses into SMC and activates the soluble guanylylcyclase. The rising levels of cyclic guanosine monophosphate (cGMP) activate the Rho kinase, which triggers a vasodilatory and an anti-proliferative effect (20-21). This cascade is limited by the phosphodiesterase-5 (PDE-5) in PASMC, which catabolizes cGMP to guanosine monophosphate. Nitric oxide itself has a short half-life since it reacts with oxygen (22) inside the PASMC. Pulmonary arterial endothelial cell (PAEC), isolated from IPAH patients, show reduced NO production in comparison to healthy controls (23).

1.3.2.2 Platelet derived growth factor

Since PAH is characterized by the increased proliferation of cells building the vascular wall, there is a plethora of growth factors and their downstream targets that were found to be deregulated in this pathological condition. Platelet derived growth factor (PDGF) is a potent growth factor and it is synthesized by many cells and in particular, by platelets, endothelial and epithelial cells. Depending on the tissue type, PDGF isoforms, PDGF A, PDGF B, PDGF C and PDGF D, are synthesized and subsequently assembled to dimers, such as PDGF-AA or PDGF-BB (24). The most investigated isoform of PDGF is PDGF-BB which activates a dimeric platelet derived growth factor receptor β (PDGFRβ) and triggers cell proliferation, migration and cell differentiation. There are many downstream

mediators of the PDGFRβ including IP3 kinase, mitogen activated-protein kinases and signal transducer and activator of transcription 3, among others (25).

A vital PDGF activation is essential in embryogenesis, while a dysregulation of the activity of this growth factor may contribute to the pathogenesis of hyper-proliferative diseases such as leukemia, cancer and PAH.

In PAH, the expression of PDGFRβ is upregulated in PASMC and PAEC, while the expression of PDGF-BB is exclusively increased in PAEC (26). PASMC, stimulated with PDGF-BB, proliferate in an ERK1/2 dependent manner and inhibition of PDGF-BB signaling by STI571, reverses this effect (27). STI571 (also known as Imatinib) is one of the first tyrosine kinase inhibitors blocking the effects of PDGFRβ. In general, Imatinib administration to rats, that were treated with monocrotaline (MCT), attenuates PH in comparison to vehicle-treated animals (28). Imatinib application improves in MCT-treated rats right ventricular systolic pressure (RVSP), which correlates with the mPAP, and improves cardiac index, a parameter of cardiac function. Moreover, Imatinib was used in a hypoxia/SU5416 mice model, which combines hypoxic exposure with the inhibition of vascular endothelial growth factor receptor (VEGFR) by the tyrosine kinase inhibitor SU5416 (Semaxanib). Mice exposed to hypoxia and treated with SU5416 develop more sever PH in comparison to mice that are only exposed to hypoxia (29). Ciuclan *et al.* reported that the administration of Imatinib into hypoxia/SU5416-exposed mice attenuates PH in comparison to control animals (30). Right ventricular systolic pressure and cardiac function were also ameliorated in Imatinib treated hypoxia/SU5416 mice. Despite these successful preclinical studies, clinical trials showed that the application of Imatinib is associated with severe adverse effects and only moderate improvements of a 6-minute walking distance (6-MWD) (31). Consequently, Imatinib is not recommended by the current guidelines for the treatment of PH. However, Imatinib is approved for the treatment of chronic myeloid leukaemia and gastrointestinal tumors (32).

1.3.2.3 Metabolic shift in vascular cells in PAH

Metabolism's alterations of a cell are associated with several diseases such as cancer, atherosclerosis and diabetes (33). In PAH, changes in the metabolism of PAEC and PASMC are similar to those observed in cancer. Glucose metabolism plays a central role in those disorders because glucose can be metabolized in different ways: by oxidative phosphorylation, which relies on the oxidation of intermediates of glucose in the mitochondrion; by anaerobic glycolysis, which describes the conversion of glucose to lactate under hypoxic conditions and by aerobic glycolysis, which also describes the conversion of glucose to lactate but under normoxic conditions (34). Physiologically, cells

are rather dependent on oxidative phosphorylation, when oxygen is available and on glycolysis under hypoxic conditions (35). Oxidative phosphorylation of glucose yields a higher amount of adenosine triphosphate (ATP), in comparison to aerobic glycolysis. However, aerobic glycolysis provides more ATP in total than oxidative phosphorylation because aerobic glycolysis is more rapid than oxidative phosphorylation (36). Regarding the pro-proliferative effect, aerobic glycolysis provides intermediates for cell proliferation. Aerobic glycolysis was described for the first time in 1930s in cancer cells and was called the Warburg effect. There are many reports showing that aerobic glycolysis takes place when mitochondrial damage occurs. Excessive activation of hypoxia induced factor-1α (HIF1-α), observed under these conditions, results in the upregulation of glycolytic enzymes and in the inhibition of pyruvate dehydrogenase which is a key enzyme in the process of oxidative phosphorylation (37,38). PAEC as well as PASMC are described to change their glucose metabolism towards an aerobic glycolysis in the context of PAH (23, 38).

1.4 Diagnostic tools in PH

The symptoms of PAH are unspecific and this makes a clinical diagnosis difficult. Thus, PAH is mostly diagnosed when other cardiopulmonary disorders have been excluded. First of all, patients are subject to physical examination that gives an overview of the patient's state and capability and during this examination signs of right heart overload can be discovered. For example, the filling of the external jugular vein reflects the function of the right heart and overloaded jugular veins can be frequently observed in the patient suffering from right heart overload. Physiologically, the external jugular vein collapses during inspiration in an upright position of the patient. An overload of the right heart impairs a collapse of the jugular vein or even increases the filling (39).

Concerning heart auscultation, a heart murmur is frequently audible with a punctum maximum above the tricuspid valve. This murmur represents the tricuspid regurgitation which is due to the right ventricle overload. The echocardiographical examination is a helpful non-invasive tool to screen for PAH and to further evaluate the progression of the disease. A right heart overload, which is pivotal in PAH and other PH types, can be examined by several parameters (40):

1. The measurement of the right atrial area and the diameter of the pulmonary artery are the parameters that are easy to assess. Due to the right heart overload, the right heart chambers and the pulmonary artery are dilated, so that increased values can give hints of an existing PH.

2. With the help of the Doppler-method flows inside the heart can be measured. By examining the peak flow of tricuspid regurgitation and adding it to the estimated right

atrial pressure, the mPAP can be approximately calculated (41). However, this indirect measurement of the mPAP is not accurate and often complemented by an invasive right heart catheter measurement. The mPAP evaluation by echocardiography serves only as a guide value if patients exhibit PH symptoms (42). Other parameters are the tricuspid annular plane systolic excursion and tricuspid insufficiency peak gradient (40). The exact value of mPAP, however, is of great interest because of the correlation between the mPAP and stage of PAH. Currently, mPAP can only be assessed by right heart catheterization (RHC) which is an invasive procedure and needs a strict indication. Despite its invasiveness, RHC is still considered as a gold standard for the diagnosis of PAH (43) and other PH types. RHC permits not only the precise measurement of the mPAP, but it also allows the measurement of other important parameters including cardiac output, a parameter reflecting heart function and pulmonary artery wedge pressure. The latter is used to diagnose PH due to left heart insufficiency (5). In addition, genetic analysis of patients, suffering from PAH, gains importance. For instance, the mutation in bone morphogenetic protein receptor type 2 (BMPR2), endoglin and activin receptor like type 1 (ALK1) genes are associated with susceptibility of developing PAH (44,45). In general, ALK1, BMPR2 and endoglin mutation are autosomal dominant with a low penetrance and can be passed on descendants or can occur as *de novo* mutations. In terms of BMPR2 loss of function mutation, it was reported that BMPR2 dysfunction is associated with poor survival of PAH patients (44). Thus, the sequencing of BMPR2 gene in PAH patients may help to estimate prognosis and can also offer new therapeutic approaches.

1.5 Therapy of PH

The therapy of PH strongly depends on the WHO PH group and sometimes it is sufficient to treat the underlying disorder, such as heart insufficiency or COPD, in order to diminish PH.

1.5.1 Pharmacotherapy

Pulmonary arterial hypertension has its own specific medical therapy. This includes vasoactive drugs such as ET-antagonists, PDE-5 inhibitors and PGI_2 analogues. ET antagonists either block the ET_A, the receptor expressed by PASMC only, or dually block ET_A- and ET_B- receptors. They decrease the vasoconstriction of pulmonary vessels and attenuate the proliferation of PASMC. PDE-5 inhibitors maintain the effect of cGMP, the second messenger of the vasodilatory agent NO, by inhibiting its degradation to inactive GMP. Like the ET antagonists, PDE-5 inhibitors decrease vasoconstriction and diminish PASMC proliferation. The principle of action of PGI_2 analogues do not differ from ET

antagonists and PDE-5 inhibitors. They also support vasodilation and improve the same clinical parameters such as 6 MWD, cardiac output and survival (1). Other pharmacological agents used in the treatment of PAH are Ca^{2+} channel blockers (CCB) which inhibit intracellular Ca^{2+} influx in PASMC leading to a vasodilation. Ca^{2+} channel blockers are predominantly used if patients show a positive vasoreactivity test (1, 46). Vasodilation caused by PDE-5 inhibitors, CCB and PGI_2 analogues also accounts for adverse effects such as headache or epistaxis in PAH patients. The European guideline of PH recommends the treatment for PAH with CCB, in case of a positive vasoreactivity test, and otherwise a therapy with an ET antagonist and a PDE-5 inhibitor is recommended. Additionally, the therapy can be complemented by PGI_2 analogues. However, the current therapeutic strategy is still not sufficient to control or cure PAH, so that there are many drugs which are tested in clinical trials. Bardoxolone, a nuclear factor E2-related factor 2 agonist with immunomodulatory properties is currently tested in phase 3 clinical trials (47). In the phase 2 LARIAT study, bardoxolone improved the 6-MWD.

A further immunomodulatory drug, tocilizumab, an interleukin 6 inhibitory antibody, tested in the therapy of rheumatoid arthritis, was also used in the phase 2, TRANSFORM-UK, clinical trial (48). The results of tocilizumab application to PAH patients in comparison to placebo group, however, show no improvement of parameters such as 6-WMD and pulmonary vascular resistance.

1.5.2 Non-medical and surgical interventions

It is recommended for PAH patients to perform light exercise which should be adapted to their symptoms. Patients who were frequently active show an improved 6MWD, less sever or milder symptoms and a better cardiac output (49). Due to the susceptibility to pneumonia, PAH patients are recommended to obtain vaccination against pathogens causing pneumonia such as influenza (1). Surgical interventions are used in advanced stages of the disease and when other therapeutic options turned out to be insufficient. A balloon septostomy is able to relieve the right heart from further overload by allowing blood to bypass lung circulation and directly reach the left heart. This intervention can, despite low blood oxygenation, improve to a certain extent the quality of life of PH patients

The ultima ratio intervention and only curative treatment available for PAH is a lung transplantation. However, this procedure as well as following effects restrict the life quality of the patients. First of all, patients who underwent lung transplantation, show a 5-year survival of only 60% (50). Immunosuppression, which needs to be maintained for lifetime in these patients, worsens or induces further disorders such as arterial

hypertension, diabetes mellitus, kidney insufficiency and cancer (50,51). Moreover, lung transplanted patients are more susceptible to infections. Due to these adverse effects, lung transplantation is reserved for exceptional cases.

1.6 Low density lipoprotein receptor-related protein 1 (LRP1)
1.6.1 Structure and function of LRP1

Low density lipoprotein receptor-related protein 1 (LRP1) belongs to the LDL receptor family. It works as a scavenger receptor and signaling receptor. Hepatocytes, smooth muscle cells, neuronal cells and also to a lesser extent endothelial cells, express this protein. LRP1 consists of a heavy α-chain with a molecular weight of 515 kDa and of a light β-chain with a molecular weight of 85 kDa (52). The heavy chain is located in the extracellular space, binds up to 100 different ligands and it is non-covalently connected to the light chain at the cell surface. The β-chain consists of a cytoplasmatic and an extracellular portion. The cytoplasmatic portion, also known as the intracellular domain (ICD) of LRP1, works as a binding site for signaling molecules and can be phosphorylated under certain conditions (53). Moreover, intramembranous LRP1 can be cleaved by a gamma secretase, the ICD of LRP1 is then released into the intracellular space and modulates gene expression by getting transferred to the nucleus (54).

The modulation of the signaling pathways by LRP1 has been reported previously. The PDGF signaling can be regulated by LRP1. Activation of the PDGFRβ leads to LRP1's cytoplasmatic tail phosphorylation at the NPxY motif (55). This phosphorylation facilitates the binding of proteins that possess a phosphotyrosine binding domain or a Src homology 2 domain. The downstream mediator of the PDGF pathway, a tyrosine phosphatase, SHP-2 (Src homology region 2-containing protein tyrosine phosphatase 2), activates several intracellular signaling pathways including the Ras/Raf and MAPK pathway. SHP-2 binds to the phosphorylated PDGFRβ, however, if LRP1's cytoplasmatic tail is also phosphorylated, SHP-2 preferentially interacts with the LRP1's tail. Thus, PDGFRβ competes with LRP1 for SHP-2. Binding of SHP-2 to LRP1 leads to the attenuation of the PDGF signaling (56-58). The transforming growth factor-β (TGF-β) pathway is also regulated by LRP1. Binding of the TGF-β to the TGF-β-receptor leads to the receptor phosphorylation and activation of its downstream targets, Smad2 and Smad3. Smad2 and Smad3 in association with Smad4 are directly responsible for the regulation of the expression of the TGF-β responsive genes. LRP1, which is also known as TGF-β receptor V, may bind TGF-β, however the binding of TGF-β to LRP1 does not trigger intracellular signaling. Thus, LRP1 functions as an inhibitory receptor for TGF-β (59).

In the context of lipoprotein metabolism, LRP1 functions as a receptor for ApoE, which belongs to lipoproteins carrying lipids and cholesterol. Binding of ApoE to LRP1 results in the uptake of the lipids and cholesterol into the cell. Moreover, LRP1 conducts the cleavage of several extracellular proteins such as matrix metalloproteinases, growth factors and extracellular matrix proteins.

1.6.2 LRP1 and its implication in vascular disorders

Atherosclerosis is defined as a vascular disease of the arteries leading to decrease of the diameter of the vessel due to plaque formation and stiffening of vascular walls. The pathogenesis of atherosclerosis is multifactorial with elevated blood lipid levels, vessel damage due to smoking and arterial hypertension contributing to the development of the disease. The consequences of atherosclerosis can be fatal as they may lead to coronary heart disease, aneurysm formation and peripheral arterial disease (60). The development of atherosclerosis involves excessive smooth muscle cell proliferation, transformation of macrophages to foam cells and endothelial dysfunction. Interestingly, LRP1 plays an important role in the maintenance of aforementioned cells. It has been reported that LRP1 depletion in SMC triggers abnormal proliferation of these cells consequently leading to the aneurysm formation (61). This effect was attenuated when mice lacking LRP1 in SMC, were treated with Imatinib. LRP1 was found to inhibit the PDGF signaling pathway by attenuating the PDGFRβ phosphorylation (61). In addition, LRP1 was reported to inhibit the TGF-β signaling in SMC (59). Macrophages, which also play a pivotal role in the pathogenesis of atherosclerosis, were also reported to be dysfunctional following LRP1 depletion. *In vivo* experiments with high fat diet fed mice showed that LRP1 depleted macrophages promote the development of a severe form of atherosclerosis as compared to control animals. Macrophages lacking LRP1 exhibit increased expression of inflammatory mediators such as monocyte chemotactic protein-1 and tumor necrosis factor-α (TNF-α). Moreover, arteries of these LRP1 knockout animals develop more lesion areas and elastic lamina breaks which represent a more advanced stage of atherosclerosis (62).

In contrast to this protective role of LRP1, lipid accumulation in macrophages and SMC is reported to be propagated by LRP1 through the uptake of low density lipoproteins (LDL) (63). An increased uptake of LDL by SMC and macrophages is associated with higher appearance of foam cells which play an important role in the development of stenosis of arterial vessels (64,65).

1.7 Physiology and plasticity of smooth muscle cells

Differentiation and phenotype plasticity are essential for a physiological SMC function. In the embryogenesis, vasculature needs to be constructed and re-arranged by the differentiation of several pluripotent stem cells. It has been described, that there are multiple progenitor cells that are capable of expressing SMC markers, such as myocardin (Myoc), α-smooth muscle actin (α-SMA) and caldesmon. For instance, the SMC of the coronary arteries derive from the proepicardium, while most of the abdominal aortas SMC arise from the splanchnic mesoderm and SMC of lung vessels originate from the pleural mesothelium (66). At this stage, these precursor cells exhibit proliferative and migratory behavior, in order to build new vessels for the developing embryo. These cells possess a synthetic phenotype and respond to PDGF-BB and TGF-β which regulate their growth and migration. PDGF-BB and TGF-β knockout mice die during their embryogenesis due to hemorrhage which results from vessel malformation (67-69). Synthetic SMC express specific pattern of proteins including matrix metalloproteinase 2 (MMP2), matrix metalloproteinase 9 (MMP9), osteopontin and fibronectin, among others (70). These proteins are essential for the function of synthetic SMC and can be considered as their marker proteins. During the maturation of vessels, the SMC are anchored in the vessel wall and start switching into a contractile phenotype. This phenotype is characterized by an expression of several contractile proteins, that are essential for vital cell contraction. Myocardin, calponin, myosin heavy chain (MHC), caldesmon and α-SMA are markers of contractile SMC. Moreover, these SMC exhibit a reduced proliferation and migration (71). The phenotype of SMC even determines the morphology of the cell, contractile SMC are elongated while synthetic SMC are more trapezoid (72).

Multiple SMC subpopulations with different phenotypes can coexist in the vessel wall. While subendothelial PASMC show a trapezoid shape and express less contractile SMC phenotype markers such as α-SMA and MHC, PASMC adjacent to the adventitia show an elongated shape with a high expression of α-SMA and MHC. Moreover, subendothelial PASMC are more susceptible to PDGF-BB stimulation in comparison to other PASMC. Interestingly, distal small pulmonary arteries consist of uniformed, contractile PASMC (73). The particular phenotype of a SMC is not its final status, the phenotype can be switched depending on the environment that SMC is exposed to. How SMC alter their phenotype has not been fully understood yet. The phenotype switching of SMC also becomes relevant, when vessels experience injuries. It has been reported, that SMC react to vessel injury immediately by switching the phenotype from a contractile to a synthetic one. This was, for example, investigated in rats, in which balloon catheter intervention led to a vessel damage. SMC reacted immediately to the injury by increasing

their proliferation. This effect was associated with downregulation of GATA6, a transcription factor, that controls the expression of Myoc, and other markers of contractile SMC (74). Phenotype switching of SMC is relevant for many disorders including atherosclerosis, coronary heart disease or PAH.

It has been reported, that in atherosclerosis SMC undergo phenotype switching by increasing their migration and proliferation. This leads to the so called neointima formation. These SMC also demonstrate a different protein expression pattern, with contractile SMC protein markers being downregulated. Moreover, the dysfunctional SMC in the neointima are involved in inflammatory processes by releasing several cytokines including TNF-α, monocyte chemoattractant protein-1 and interleukin-1β (75). In pulmonary arteries, PASMC also undergo phenotypic alterations, however the exact molecular mechanism is unknown. Yet, there are several factors that are reported to influence the phenotype of PASMC. Enolase-1 (ENO-1) was found to promote proliferative phenotype of PASMC with further changes reported in the metabolism. Contractile SMC markers, including Myoc and α-SMA were downregulated in ENO-1 overexpressing PASMC (76). Recently, it was also reported that an integrin expression pattern alters during PASMC phenotype switching. Umesh *et al.* investigated the expression of integrins in different animal models of PH. In the hypoxia mouse model α_1-, α_5-, α_8-, α_v- and β_1-integrins were altered while in the MCT rat model changes in the expression of α_1-, α_5-, α_v- and β_3-integrins were observed (77). $\alpha_v\beta_3$-integrin was found to be upregulated in PH models leading to proliferation of PASMC in a FAK/AKT dependent manner. This proliferative state of PASMC was dependent on osteoprotegerin (OPG), a receptor belonging to the TNF-α receptor family. Notably, disruption of the binding of OPG and $\alpha_v\beta_3$-integrin, attenuated PH in the hypoxia-SU5416 mice model (78).

The settings, in which PASMC are embedded in, influence their phenotype, too. If PASMC are co-cultured with PAEC, the expression of the markers of the contractile phenotype such as MHC and calponin is raised and the morphology is altered from a rhomboid to an elongated one (79). Altogether, phenotype plasticity of SMC is essential for the adaption to environmental changes either in embryogenesis or in the pathogenesis of vascular disorders.

2. Aim of the study

The purpose of this study was to elucidate the importance of LRP1 in PASMC phenotype switching and thus, the possible involvement of LRP1 in vascular remodeling observed in PH.

3. Materials and Methods

3.1 Materials

3.1.1 Equipment

Camera	Sony, Tokio, Japan
Centrifuge Rotina 35	Hettich, Tuttlingen, Germany
Centrifuge Mikro 22R	Hettich, Tuttlingen, Germany
Cell counter TC-10	Bio-Rad, München, Germany
Cell culture incubator MCO 15-AC	Sanyo, Osaka, Japan
Cell culture insert, 8.0 µm	Falcon, Corning, NY
Cell culture plates 6er, 24er	Sarstedt, Nümbrecht, Germany
Chemidoc Imaging	Bio-Rad, München, Germany
ELISA plate reader SpectraMax 190	Molecular devices, Biberach, Germany
Filter tips	Eppendorf, Hamburg, Germany
Gel blotting paper	Roth, Karlsruhe, Germany
Microscope	Leica, Wetzlar, Germany
Pipets	Gilson, Middleton, WI
Pipette controller, Pipetboy	Integra, Biebertal, Germany
PCR thermocycler	Biometra, Goettingen, Germany
Petri dish	Sarstedt, Nümbrecht, Germany
PDVF membrane	Roth, Karlsruhe, Germany
Real-time PCR machine SteponePlus	Applied Biosystems, Forster City, CA
Laminar flow	Thermo Scientific, Waltham, MA
Shaking incubator	Peqlab, Erlangen, Germany
Specimen slide	Roth, Karlsruhe, Germany
Vortex machine, Vortex-Genie 2	Scientific industries, Bohemia, NY
Water bath	GFL, Burgwedel, Germany
Western blot chambers	Bio-Rad, München, Germany

3.1.2 Reagents

2-mercapto-ethanol	Sigma-Aldrich, St. Louis, MO
Acetone	Roth, Karlsruhe, Germany
Acetic acid	J.T. Baker, Deventer, The Netherland
Acrylamide	Roth, Karlsruhe, Germany
Agarose	Roth, Karlsruhe, Germany
Bovine serum albumin	Sigma-Aldrich, St. Louis, MO
Dimethyl sulfoxide	Roth, Karlsruhe, Germany
DMEM	Gibco, Carlsbad, CA
DMEM/F12	Gibco, Carlsbad, CA
ECL western blot detection reagent	GE Healthcare, Buckinghamshire, UK
Ethanol	Roth, Karlsruhe, Germany
Ethidium bromide	Sigma-Aldrich, St. Louis, MO
Ethylendiamintetraacetat (EDTA)	Sigma-Aldrich, St. Louis, MO
Fetal calf serum	Hyclone, South Logan, UT
Glycine	Roth, Karlsruhe, Germany
Guanidiniumthiocyanat	Roth, Karlsruhe, Germany
HEPES	Roth, Karlsruhe, Germany
High-capacity cDNA reverse transcription kit	Invitrogen Life Technologies, Carlsbad, CA
LDH Cytotoxicity Detection Kit	Roche, Mannheim, Germany
Methanol	Roth, Karlsruhe, Germany
Methyl-^{3}H-thymidine	PerkinElmer Life Sciences, Waltham, MA
Milk powder, low fat	Roth, Karlsruhe, Germany
Opti-MEM™	Gibco, Carlsbad, CA
peqGOLD total RNA kit	Peqlab, Erlangen, Germany
PageRuler™ plus prestained protein ladder	Thermo Scientific, Waltham, MA
Penicillin/Streptomycin	Invitrogen Life Technologies, Carlsbad, CA
Pierce ECL western blotting substrate	Thermo Scientific, Waltham, MA
Pierce BCA protein assay kit	Thermo Scientific, Waltham, MA
Platinum™SYBR™ green qPCR supermix	Invitrogen Life Technologies, Carlsbad, CA
Potassium chloride	Roth, Karlsruhe, Germany

RPMI	Gibco, Carlsbad, CA
Smooth muscle cell medium, SMC Vasculife	Cell Systems, Troisdorf, Germany
Sodium chloride	Roth, Karlsruhe, Germany
TEMED	Merck Millipore, Burlington, MA
Tris, powder	Roth, Karlsruhe, Germany
Triton X-100	Sigma-Aldrich, St. Louis, MO
Tween 20	Sigma-Aldrich, St. Louis, MO
Trypsin/EDTA	Merck Millipore, Burlington, MA
Water, sterile	Braun, Melsungen, Germany

3.2 Methods

3.2.1 Human material

The investigations were conducted in accordance with the Declaration of Helsinki principles and were approved by the local institutional review board and ethics committee. Informed consent was obtained from either the patients or their next-of-kin. Lung tissue was obtained from 24 IPAH patients who underwent lung transplantation at the Department of Cardiothoracic Surgery, Medical University of Vienna, Austria. Non-utilized donor lungs (n=28) served as a control. Patient and donor characteristics are summarized in Table 1.

Table 1. IPAH patients and donor characteristics for lung tissue samples.

	IPAH (n=24)	Donor (n=28)
Age (mean±SD)	41,7±10,8	43,9±8,5
Sex (female/male; %)	72/28	67/33
mPAP (mmHg)	51,9±18,8	-
NYHA classification	III-IV	-

IPAH; idiopathic pulmonary arterial hypertension, mPAP; mean pulmonary arterial pressure, NYHA; New York Heart Association

3.2.2 Animal experiments

All animal experiments were performed in accordance with institutional and national guidelines for the care and use of experimental animals. For hypoxic exposures, male wild type mice (10 weeks old) were placed in a ventilated chamber system with a FiO_2 of 0.10. To induce PH in rats, male Sprague-Dawley rats were injected with 60 mg/kg monocrotaline (MCT) by a single application of MCT in the area near of animal neck. STI571 (Imatinib/Gleevec®, Novartis, Basel, Swiss) administration in rats was conducted by a once-daily intraperitoneal injection (50 mg/kg), control animals received isotonic saline (50 mg/kg) instead. Mice were fed with either STI571 or placebo orally after 21 days of hypoxic or normoxic exposure. After 28 days, MCT-injected rats and mice-exposed to hypoxia were sacrificed and lung tissue samples were prepared for further analysis. Histological lung tissue samples kindly provided by Dr. Kwapiszewska and Dr. Schermuly were used in this doctoral work.

3.2.3 Isolation and culture of PASMC

Pulmonary artery smooth muscle cells (PASMC) used for all the experiments were isolated from non-utilized human donor lungs (lungs harvested for lung transplantation that were not implanted due to lack of compatibility) or from IPAH patient lungs. The cells were isolated from human pulmonary arteries (from the third intrapulmonary branch, diameter <1mm). PASMC were cultured in Vasculife SMC Medium Complete Kit (Lifeline Cell Technology, Oceanside, CA) supplemented with 10 mM L-Glutamine, 5% fetal bovine serum (FBS), 5 ng/mL recombinant human (rh) epidermal growth factor, 5 µg/mL rh insulin, 50 µg/mL ascorbic acid, 5 ng/mL rh fibroblast growth factor-b (all from Lifeline Cell Technology) and 1% Penicillin/Streptomycin (Invitrogen Life Technologies, Carlsbad, CA). The cells were cultured at 37°C in a humidified incubator with 5% CO_2.

3.2.4 siRNA transfection and treatment of PASMC

PASMC were transfected with 100 nM siRNA at 60-70% confluence using Lipofectamine® 2000 (Thermo Fisher Scientific, Darmstadt, Germany) dissolved in Opti-MEM™ and analyzed 48h thereafter. siRNA directed against human LRP1 (sense strand 5'-CCUGUAACCUGCAGUGCUUdTdT-3') was synthesized by Microsynth AG (Lindau, Germany) and the control siRNA was purchased from Ambion (Austin, TX). In some experiments, PASMC were treated with the following reagents: 12.5 µg/mL cycloheximide (Sigma-Aldrich, Hamburg, Germany), 10 ng/mL PDGF-BB (R&D Systems, Wiesbaden, Germany, catalog number: 220-BB-010), 2 µM Imatinib (Sigma-Aldrich, St. Louis, MO), 10 µg/mL anti- PDGF-BB neutralizing antibody (R&D Systems, catalog number: AF-220), 10 µg/mL β_1-integrin-blocking antibody (clone P5D2; Abcam, Berlin, Germany, catalog number: ab24693), 10 µg/mL β_4-integrin blocking antibody (clone ASC- 3; Millipore, Darmstadt, Germany, catalog number: MAB 2058), or 10 µg/mL respective isotype control antibody (BD Bioscience , Franklin Lakes, NJ, catalog number: 553927).

3.2.5 Protein isolation and western blotting

Proteins were isolated in a lysis buffer containing 50 mM Tris, pH 7.4, 150 mM NaCl, 1 mM EDTA, 1% Triton-X-100, 1% Sodium Deoxycholate and 0.1% SDS supplemented with 1 mM Na_3VO_4, 1 mM PMSF and 1 µg/mL Complete Protease Inhibitor Cocktail (Roche Applied Science, Indianapolis, IN), separated on a 10% SDS polyacrylamide gel and transferred to a PVDF membrane (Roth, Karlsruhe, Germany). The membrane was blocked with 1% bovine serum albumin (BSA) and treated with one of the following antibodies: rabbit anti-LRP1 (1:1000 dilution, Abcam, catalog number: ab92544), rabbit anti-α_5-integrin (1:500 dilution, Cell Signaling Technology, Leiden, The Netherlands,

catalog number: 4750P), mouse anti-α-smooth muscle actin (1:1000 dilution, α-SMA; Millipore, catalog number: CBL171), mouse anti-myocardin (1:500 dilution, R&D Systems, catalog number: MAB4028), mouse anti-fibronectin (1:250 dilution, Enzo Life Science, Loerrach, Germany, catalog number: FG-6010), goat anti-collagen I (1:1000 dilution, SouthernBiotech, Birmingham, AL, catalog number: 1310-01), mouse anti-osteopontin (1:500 dilution, Santa Cruz Biotechnology, Santa Cruz, CA, catalog number: sc-21742) and mouse anti-β_1-integrin (1:1000 dilution, Abcam, catalog number: ab24693). The membrane was incubated afterwards with a peroxidase labeled secondary antibody (1:3000, all from Dako, Glostrup, Denmark, catalog number: P0447 (mouse), P0217 (rabbit) and P0449 (goat)), dissolved in TBS-T (25 mM Tris-HCl, 150 mM NaCl, pH 7,5, 0,1% Tween 20). Proteins were detected using either Amersham ECL Select Western Blotting Detection Reagent (GE Healthcare, Chicago, IL) or Pierce ECL Western Blotting Substrate (Thermo Fisher Scientific). The pictures were acquired using a ChemiDoc Imaging Systems (Bio-Rad, Hercules, CA). α-Tubulin, detected using a rabbit-anti α-Tubulin antibody (1:1000 dilution, Cell Signaling, catalog number: 2125), was used as a loading control.

Protein extraction from microdissected formalin-fixed and paraffin-embedded tissue was conducted as followed. Tissue sections were deparaffinized by the incubation with xylene for 10 min. Subsequently, the tissue pieces were rehydrated using a graded series of ethanol (100%, 96%, 70% and 50%) and resuspended in an extraction buffer containing 20 mM Tris-HCl pH 9.0 0.2 M glycine and 2% SDS (80). The suspension was heated up to 80°C and the supernatant containing proteins was used for western blotting.

3.2.6 RNA isolation and reverse transcription (RT)

RNA was isolated from PASMC using the PeqGold Total RNA kit according to the manufacturer's instruction. Afterwards, RNA was converted into cDNA using the High Capacity cDNA reverse transkriptase kit (Applied Biosystems). Reagents and their volume are presented in table 2.

Table 2. Composition of the master mix for RT reaction.

Master mix	Volume (µL)
MultiScribe ™ reverse transcriptase (50 U/µL)	1.0
10x reverse transkriptase buffer	2.0
10x random primer (25 µM)	2.0
Desoxynucleoside triphosphate (100 mM)	0.8
RNase inhibitor (20 U/µL)	0.5
RNase free water	3.7

The reaction was conducted using a thermocycler. PCR conditions are presented in table 3. Afterwards, the samples were stored at -20°C.

Table 3. Cycle conditions of RT reaction.

Cycle	1	2	3	4
Temperature (°C)	25	37	85	4
Time (min)	10	120	5	∞

3.2.7 Quantitative PCR

Quantitative PCR (qPCR) was conducted using the Platinum Sybr Green qPCR Super Mix (Applied Biosystems) according to the manufacturer's instruction. The composition of the master mix is presented in table 4 and the cycling conditions of the qPCR reaction are described in table 5.

Table 4. Master mix used for qPCR.

Master mix	Volume (µL)
Reverse primer (5 µM)	1.0
Forward primer (5 µM)	1.0
cDNA	1.0
$MgCl_2$ (25 mM)	1.0
Sybr green mix	13.0
RNase free Water	8.0

Table 5. Cycling conditions of qPCR.

	Denaturation		Cycling stage (40x)		
			Denaturation	Hybridization	Elongation
Temperature (°C)	50	95	95	59	72
Time (s)	120	300	5	5	30

Reverse and forward primers that were used for all experiments are presented in table 6. Porphobilinogen deaminase (PBGD) was used as a reference gene. Changes in gene expression are reported as ΔCt ($Ct_{(PBGD)} - Ct_{Gen\ of\text{-}interest\ (GOI)}$). Values calculated in this way are proportional to the -log normalized amount of the GOI. In order to check for exclusive amplification of a qPCR product, melting-curve analysis and gel electrophoresis were performed. Alternatively, gene expression was analyzed using the Extracellular Matrix and Adhesion Molecules RT2 Profiler PCR Array (Qiagen, Hilden, Germany) according to the manufacturer's instructions. Changes in RNA expression of each target gene were normalized using averages of Ct values of the following reference genes: β-actin, β_2-microglobulin, glyceraldehyde-3-phosphate dehydrogenase, and hypoxanthine phosphoribosyltransferase. Changes in a target gene expression are reported as $\Delta\Delta Ct$ ($Ct_{average\ of\ reference\ genes} - Ct_{GOI}$) $_{siLRP1} - (Ct_{average\ of\ reference\ genes} - Ct_{GOI})$ $_{siCtrl}$ from 3 biological replicates.

Table 6. List of primers used for qPCR:

Gene	Accession number	Nucleotide sequence (5'->3')	T_m[1] (°C)	Amplicon size (nt)[2]
Human *LRP1*	NM_002332.2	F[3]: 5'-TCTACTTTGCCGACACCACC-3' R[4]: 5'-TGTCTTTTTGGGCCCATCGT-3'	89	160
Human *ITGB1*	NM_002211.4	F: 5'-CCGCGCGGAAAAGATGAA-3' R: 5'-CACAATTTGGCCCTGCTTGTA-3'	81	150
Human *ACTA2*	NM_001613.4	F: 5'-GTGTTGCCCCTGAAGAGCAT R: 5'-CGCCTGGATAGCCACATACAT-3'	81	130
Human *MYOCD*	NM_153604	F: 5'-AGGTAACACAGCCTCCATCCT-3' R: 5'-TCTAGCGTCTGCTGGCATTT-3'	83	118
Human *FN1*	NM_212482.3	F: 5'-CACCTCTGTGCAGACCACATC-3' R: 5'-GTCTCTTGGCAGCTGACTCCG-3'	85	215
Human *SPP1*	NM_001040058.2	F: 5'-GAAGATGATGATGACCATGTG-3' R: 5'-GTCAGGTCTGCGAAACTTC-3'	81	263
Human *HMBS*	NM_000190.4	F: 5'-ACCCTAGAAACCCTGCCAGAGAA-3' R: 5'-GCCGGGTGTTGAGGTTTCCCC-3'	88	69
Rat *Lrp1*	NM_001130490.1	F: 5'-CGTCACTTACATCAACAACC-3' R: 5'-CAGCCATTCACATTTCTTGC-3'	88	165
Rat *Hmbs*	NM_013168.2	F: GCCAGAGAAAGTGCCGTGGGG-3' R: 5'-CCAGCTTCCGTAGGCGGGTG-3'	87	121
Murine *Lrp1*	NM_008512.2	F: 5'-CGCCTGTGAGAATGACCAGT-3' R: 5'-TCTAATGATGCCTGGGC-3'	89	192
Murine *Hmbs*	NM_013551.2	F: 5'-GCCAGAGAAAGTGCCGTGGG-3' R: 5'-TCCGGAGGCGGGTGTTGAGG-3'	87	115

[1]Tm, melting temperature, [2] nt, nucleotide, [3]F, forward, [4]R, reverse, LRP1, Low density lipoprotein receptor-related protein; ITGB1, β$_1$-integrin; ACTA2, α-smooth muscle actin; MYOCD, myocardin; FN1, fibronectin; SPP1, osteopontin; HMBS, hydroxymethylbilane synthase

3.2.8 Analysis of microRNA103/107

Total RNA was isolated from PASMC using the TRIZOL reagent according to the manufacturer's instruction (Invitrogen Life Technologies). Afterwards, DNA digestion was performed with TURBO DNA-free™ Kit by adding 1 µL TURBO DNase™ enzyme (2 U/µL) to the RNA for 30 min. TURBO DNase™ enzyme was then inactivated by a DNase inactivation reagent, the sample was centrifuged and supernatant containing the RNA was used for cDNA synthesis.

1 µg RNA was reverse transcribed in the reaction containing 50 nM stem-loop RT primer each (microRNA103: 5'-GTCGTATCCAGTGCAGGGTCCGAGGTATTCGCACTGGAT-ACGACTCATAG-3' and microRNA107: 5'-GTCGTATCCAGTGCAGGGTCCGAGGTAT-TCGCACTGGATACGACTGATAG-3'), 2 µL 10x RT buffer, 4 mM dNTP mix, 2.5 U/µL MultiScribe Reverse Transcriptase, 1 U/µL RNase Inhibitor (all from Applied Biosystems, Waltham, MA) in a volume of 20 µL. The RT reaction was carried out at 16°C for 30 min, at 42°C for 30 min and at 85°C for 5 min. The following controls were included: no-RNA, no stem-loop RT primer, and no reverse transcriptase. MicroRNA103/107 levels were measured using SYBR Green qPCR Master Mix (Applied Biosystems) according to the manufacturer's instruction. All primers were used in the final concentration of 200 nM and the sequences were as followed: microRNA103/107 forward: 5'-CACGCAAGCAGCATTGTA-3' (recognizes microRNA103 and microRNA107) and reverse 5'-GTGCAG GGTCCGAGGT-3' and ribosomal protein lateral stalk subunit P0 (RPLP0) forward: 5'-CCTTCTCCTTTGGGCTGGTCATCCA-3' and reverse 5'-CAGACACTGGCAACATTGCG-GACAC-3'. Ribosomal protein lateral stalk subunit P0 (RPLP0) was used as a reference gene. The reaction mix was incubated at 95°C for 10 min, followed by 40 cycles of 95°C for 15s and 60°C for 60s. Melting curve analysis and gel electrophoresis were performed to confirm the exclusive amplification of the expected qPCR product. Changes in microRNA103/107 expression are presented as ΔCt (Ct_{RPLP0} – $Ct_{microRNA103/107}$).

3.2.9 Cell surface biotinylation

Cell surface proteins were labeled with 0.5 mg/mL EZ-LinkTM Sulfo-NHS-SS-Biotin (Thermo Fisher Scientific) for 1h at 4°C. After quenching with 100 mM glycine, protein isolation was performed as described above. Hundred µg biotinylated proteins were incubated with PierceTM NeutrAvidinTM Agarose beads (Thermo Fisher Scientific) overnight at 4°C. Following extensive washing with buffers containing 50 mM TRIS, pH 7.4, 5 mM EDTA and increasing concentration of NaCl (150-500 mM), the proteins were analyzed by western blotting.

3.2.10 Flow cytometry

PASMC were trypsinized and fixed with 2% paraformaldehyde for 10 min at room temperature. Afterwards, the cells were washed with phosphate-buffered saline (PBS, 137 mM NaCl, 2.7 mM KCl, 10 mM Na_2HPO_4, 2 mM KH_2PO_4, pH 7.4), blocked with 1% BSA for 1h at room temperature and surface-labeled with a rat anti-β_1-integrin (1:100 dilution; clone 9EG7; BD Biosciences, catalog number: 553715) or an isotype control (1:100 dilution, BD Bioscience, catalog number: 563039) antibody overnight at 4°C. Subsequently, the samples were washed and incubated with a fluorescein isothiocyanate (FITC)-labeled secondary antibody (1:100 dilution, Jackson Immunoresearch, Cambridge, United Kingdom, catalog number: 212-095-168) for 2h at 4°C. Flow cytometry was carried out with Accuri C6 flow cytometer and the data was analyzed using CFlowPlus (BD Biosciences) software.

3.2.11 Proliferation assay

PASMC proliferation was measured by ^{3}H-thymidine incorporation. Forty-eight h after seeding onto a 48-well-plate (2×10^3 cells/well), 0.6 µCi/mL ^{3}H-thymidine (PerkinElmer Life Sciences, Waltham, MA) in growth medium supplemented with 5% FCS was applied to the cells for 20h. Following extensive washing with PBS and cell solubilization in 0.5 M NaOH, ^{3}H-thymidine content was quantified by liquid scintillation spectrometry (Beckman LS 6500, Fullerton, CA).

3.2.12 Transwell migration assay

Cell migration was tested using polycarbonate membrane transwell inserts (8 µm pore size, BD Biosciences) coated with 2 µg/mL human fibronectin (FN) (Sigma-Aldrich) overnight at 4°C. PASMC (1×10^4) resuspended in 350 µL serum-free medium were added to the upper chamber of the transwell. Next, 350 µL of medium containing 5% FCS was applied to the bottom chamber and the cells were allowed to migrate through the membrane for 24h. Afterwards, the cells from the upper chamber were removed using a cotton swab and the cells that migrated through the membrane were fixed with a methanol/acetone solution, stained with crystal violet and counted under the microscope.

3.2.13 Adhesion assay

For cell adhesion analysis, 1×10^4 cells were seeded onto a 96-well-plate coated with 2 µg/mL human FN (Sigma-Aldrich). After 40 min incubation at 37°C, the cells were fixed with cold methanol/acetone solution (1:1) for 1h at 4°C, dried and subsequently stained with crystal violet (Sigma-Aldrich) (1:100 dilution in H_2O with 2% Ethanol). Afterwards,

the cells were lysed using 10% acetic acid. The absorbance was measured at 560 nm with a microplate reader (SpectraMax 190, Molecular Devices, Biberach, Germany).

3.2.14 Generation of Acta2-cre/ERT2; Lrp1^{flox/flox} mice

Transgenic mice expressing a tamoxifen-inducible Cre recombinase under the Acta2 promoter (B6;Tg(Acta2-cre/ERT2)12Pcn (81) were crossed with mice bearing floxed allele of Lrp1 gene (Lrp1<tm2Her>/J (82). The resulting mouse strain (B6;Tg(Acta2-cre/ERT2)12Pcn; Lrp1<tm2Her>/J, referred to herein as Acta2-Cre^{ERT2}; Lrp1^{flox/flox}) was then back-crossed for eight generations to C57BL/6J background and used for the experiments. Littermates that were homozygous for the floxed Lrp1 allele but did not carry Acta2-Cre^{ERT2} cassette (Lrp1^{flox/flox}) were used as controls.

3.2.15 Precision cut lung slices (PCLS)

PCLS were prepared from Acta2-Cre^{ERT2}; Lrp1^{flox/flox} and Lrp1^{flox/flox} mice sacrificed by cervical dislocation and exsanguinated by transection of the arteria renalis. The trachea was cannulated with a Vasofix® Safety intravenous catheter (Braun, Melsungen, Germany) and 2.5 mL of 1.5% low-melting point agarose dissolved in serum-free DMEM was injected into the lungs. After 5 min, the lungs were removed and tissue cores of a diameter of 8 mm were prepared using a sharp rotating metal tube. Subsequently, the cores were sliced into 300-350 µm thin slices in DMEM using a Krumdieck tissue slicer (Alabama Research and Development, Munford, AL). PCLS were washed 3x for 30 min in DMEM supplemented with 100 U/mL penicillin, and 100 µg/mL streptomycin (both from Biochrom, Berlin, Germany) and used for the experiments. To induce *Lrp1* gene inactivation, PCLS were treated with 5 µM 4-hydroxy tamoxifen (4-OH TXN; Cayman Chemical, Hamburg, Germany) dissolved in ethanol for 48h. Viability of the tissue was assessed by the LDH Cytotoxicity Detection Kit (Roche, Mannheim, Germany) according to the manufacturer's instruction.

3.2.16 Immunohistochemistry

Lung tissue specimens were fixed with 4% paraformaldehyde in PBS and embedded in paraffin. One µm sections were deparaffinized in xylene and rehydrated through grade ethanol washes. Antigen retrieval was achieved by cooking tissue sections in Decloaker Reagent (Zymed Laboratories Inc., San Francisco, CA) for 20 min. After cooling, tissue sections were blocked with 10% BSA in PBS for 1h and then incubated overnight at 4°C with one of the following antibodies: rabbit anti-LRP1 (1:50 dilution, Abcam, catalog number: ab92544), rabbit anti-PCNA (proliferating cell nuclear antigen) (1:50 dilution, Cell Signaling Technology, catalog number: 610665) and rabbit anti-α-SMA (1:100 dilution, Sigma-Aldrich, catalog number: A2547). Antigen detection was performed using a ZytoChem-Plus AP Polymer-Kit in accordance with the manufacturer´s instruction (Zymed Laboratories Inc.).

3.2.17 Immunofluorescence staining

PASMC from donor or IPAH lung tissue were seeded in an 8-well chamber slide (2×10^4/well) and cultured for 48h. The cells were washed with PBS, fixed with ice-cold methanol for 20 min at -20°C, permeabilized with 0.02% TritonX for 10 min, and blocked with 3% BSA in PBS for 1h. Afterwards, PASMC were incubated overnight at 4°C with mouse anti-LRP1 antibody (1:500 dilution, Abcam, catalog number: ab92544). After washing 3× with PBS, the cells were incubated with AlexaFluor 488- labeled anti-rabbit secondary antibody (1:1000 dilution, Invitrogen, catalog number: A11070) for 1h at room temperature. Finally, the slides were mounted with DAPI mounting medium (Vectashield, Vector Labs, Burlingame, CA). Images were taken using a laser scanning confocal microscope (Nikon A1R Ultra-Fast Spectral Scanning Confocal Microscope; Tokyo, Japan) with CFI Plan Apochromat Lambda 60×/1.4 oil immersion objective.

3.2.18 Statistics

Student's t-test was used for the comparison between two groups. Analysis of variance followed by Tukey's post hoc test was applied for the comparison of multiple groups. $p < 0.05$ was considered statistically significant. Data are expressed as mean ±SD of at least three independent experiments.

4. Results

4.1 LRP1 expression is upregulated in lung homogenates from IPAH patients

To assess the role of LRP1 in PH, first the distribution and expression of this receptor in human lung tissue samples was analyzed. In the lungs of patients suffering from idiopathic pulmonary artery hypertension (IPAH), strong LRP1 immunoreactivity was observed in SMC and EC of the remodeled pulmonary vessels (Figure 4.1A). In donor lungs, the pulmonary vessel wall was only weakly stained for LRP1 (Figure 4.1A). On the mRNA level there was no difference in the LRP1 expression between lung tissue samples obtained from donors and IPAH patients (Figure 4.1B), however, on the protein level marked upregulation of LRP1 expression in diseased lungs was noted (Figure 4.1C and 4.1D).
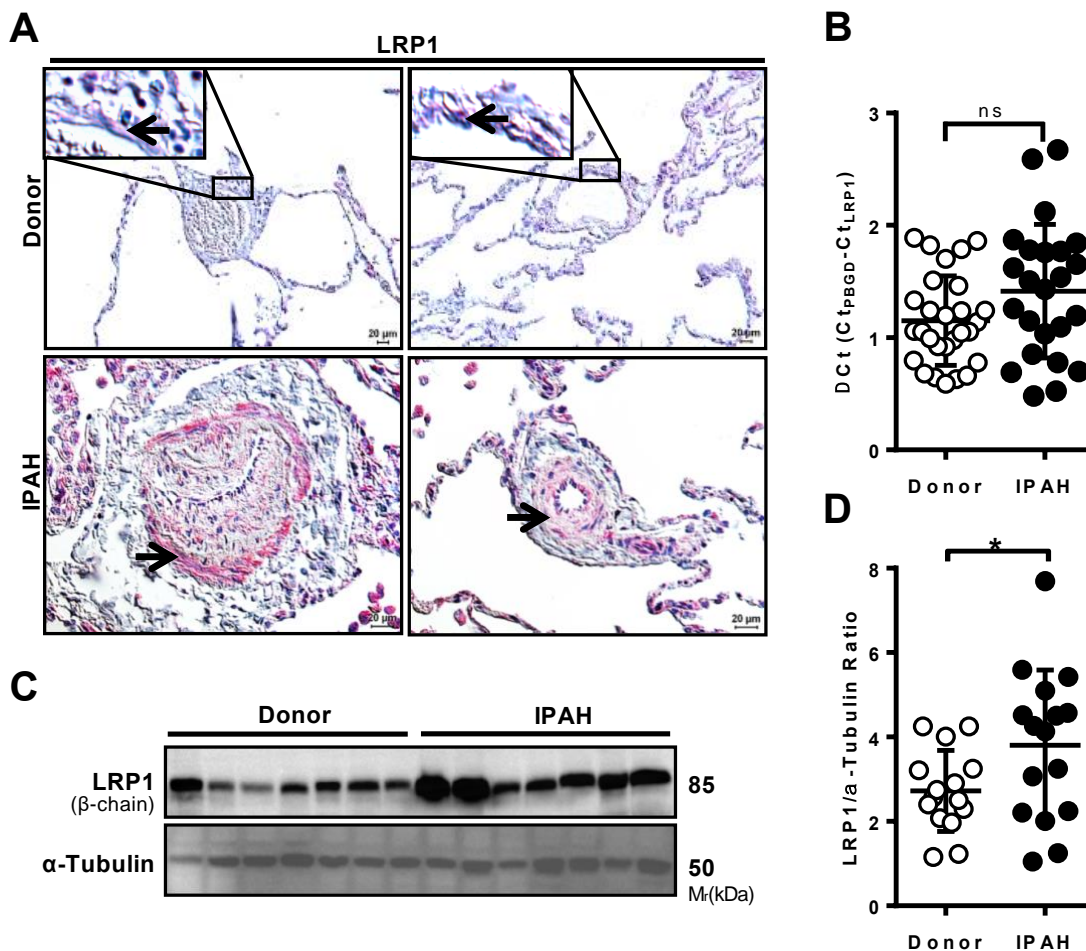
Fig. 4.1 LRP1 protein levels are increased in lungs and PASMC of IPAH patients.
(A) Immunohistochemistry for LRP1 in lungs of donors and IPAH patients. Arrows indicate media of pulmonary vessels. Scale bar = 20 µm. (B, C) LRP1 mRNA (B) and protein levels (C) in lung homogenates of donors (n=28 for RNA, n=14 for protein) and IPAH patients (n=24 for RNA, n=16 for protein). The qPCR data are presented as ΔCt using *PBGD* as a reference gene. For western blotting, α-Tubulin was used as a loading control. Representative blots are shown. (D) Densitometry analysis of (C). ns, not significant, *p<0.05.

Similarly, LRP1 mRNA levels were not changed in PASMC isolated from IPAH lungs as compared to PASMC obtained from donor lungs (Figure 4.2A), but LRP1 protein was significantly increased in IPAH PASMC as opposed to donor PASMC (Figure 4.2B and C). Immunocytochemistry conducted on PASMC isolated from donor and IPAH lungs confirmed this finding (Figure 4.2D).
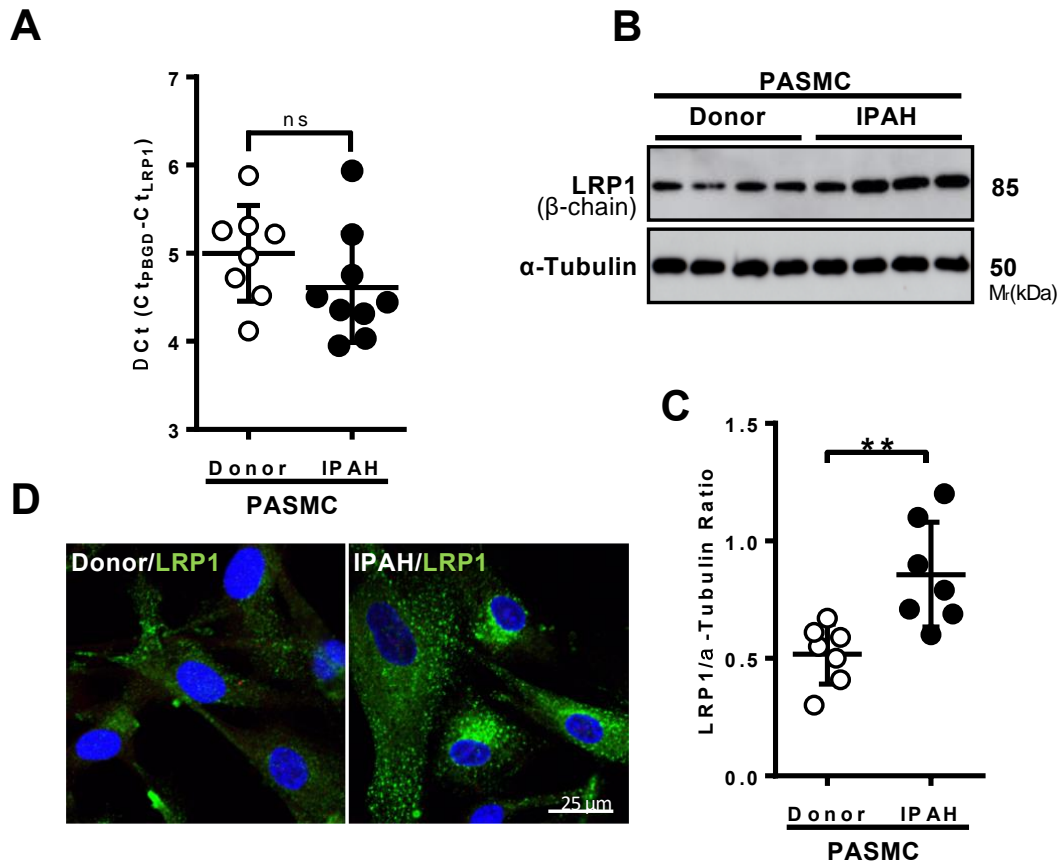
Fig. 4.2 LRP1 is upregulated in PASMC isolated from IPAH lungs.

(A, B) LRP1 mRNA (A) and protein (B) levels in pulmonary arterial smooth muscle cells (PASMC) of donors (n=8 for RNA, n=7 for protein) and IPAH patients (n=9 for RNA, n=7 for protein). The qPCR data are expressed as ΔCt using *PBGD* as a reference gene. For western blotting, α-Tubulin was used as a loading control. Representative blots are shown. (C) Densitometry analysis of (B). (D) Immunofluorescence staining for LRP1 in PASMC isolated from donor and IPAH lungs. Scale bar = 25 μm, n=7-9/group. **p<0,01; ns, not significant.

As LRP1 levels in SMC were found to be regulated by microRNA103/107 (83), the expression of these microRNAs was next analyzed in PASMC isolated from donor and IPAH lungs. However, no difference in the expression of microRNA103/107 between two experimental groups was measured (Figure 4.3A). To further explore this, cells were incubated with cycloheximide, an inhibitor of protein synthesis. As depicted in figures 4.3B and 4.3C half-life of LRP1 in donor PASMC was about 42h whereas in IPAH

PASMC was about 72h. This suggests that the increased LRP1 protein stability may account for the high LRP1 protein abundance in IPAH.
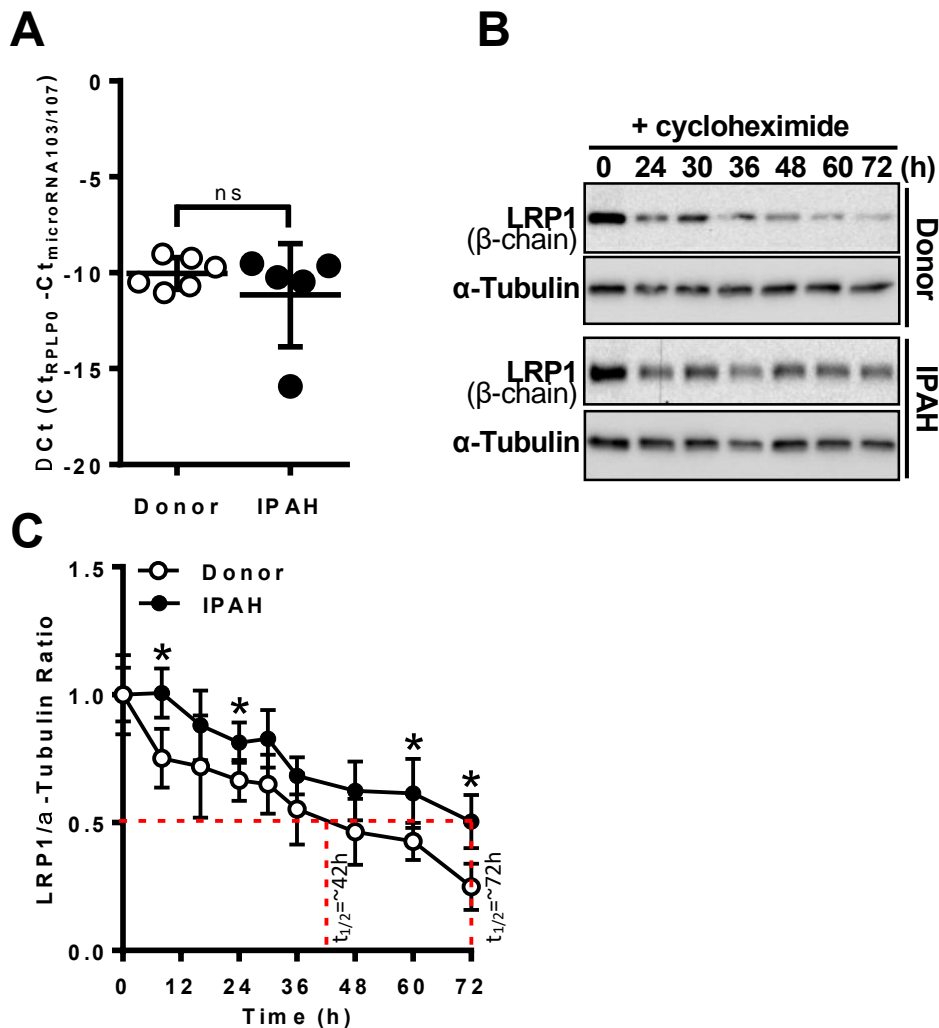
Fig. 4.3 LRP1 protein stability is increased in PASMC from IPAH patients.
(A) microRNA103/107 expression in donor (n=6) and IPAH (n=5) PASMC. The qPCR data are presented as ΔCt using *RPLP0* as a reference gene. (B) Time course of LRP1 protein stability in donor and IPAH PASMC exposed to 12.5 µg/mL cycloheximide as assessed by western blotting. α-Tubulin served as a loading control. Representative blots are shown. (C) Densitometry analysis of (B). LRP1/α-Tubulin ration at time point 0 was set to 1 (n=5). ns, not significant, *$p < 0.05$.

4.2 LRP1 expression is elevated in monocrotaline-injected rats and mice exposed to hypoxia

Next, the expression of LRP1 was analyzed in lung tissue samples obtained from experimental models of PH, rats challenged with monocrotaline (MCT) and mice maintained under hypoxic conditions (HOX). Although, *Lrp1* mRNA levels were not altered in MCT- injected rats, on the protein level strong elevation of the LRP1 expression in this experimental group was observed (Figure 4.4A-C).
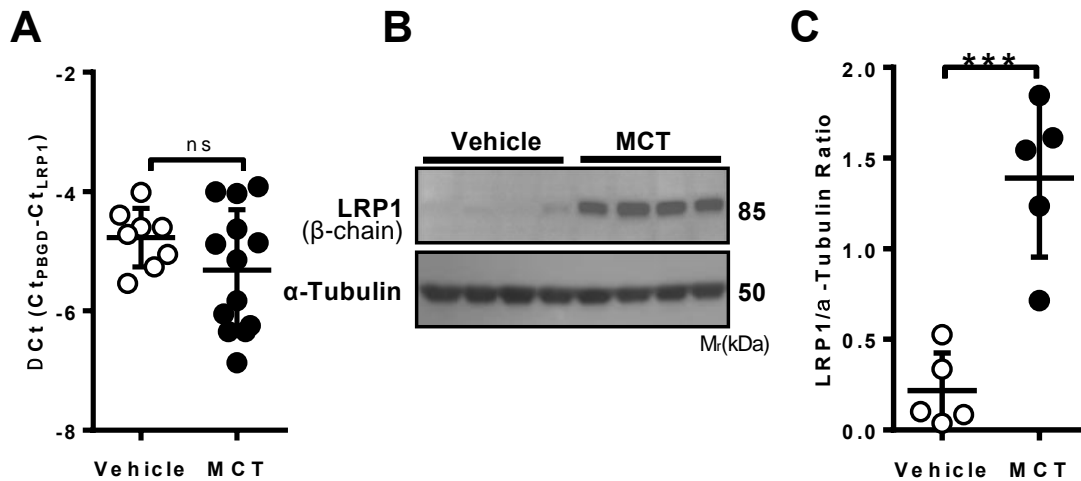
Fig. 4.4 LRP1 protein expression is upregulated in monocrotaline treated rats.

(A, B) LRP1 mRNA (A) and protein levels (B) in lung homogenates of rats treated either with vehicle (n=8 for RNA, n=5 for protein) or monocrotaline (MCT, n=13 for RNA, n=5 for protein). The qPCR data are expressed as ΔCt using *Pbgd* as a reference gene. For western blotting, α-Tubulin was used as a loading control. Representative blots are shown. (C) Densitometry analysis of (B). ns, not significant, ***p<0.001.

In mouse exposed to hypoxia, LRP1 protein (Figure 4.5 B and 4.5 C), but not *Lrp1* mRNA (Figure 4.5 A), was significantly increased. Furthermore, LRP1 staining was more intense in pulmonary vessels of HOX mice as compared to animals maintained under normoxic (NOX) conditions (Figure 4.5 D). Unfortunately, none of the antibodies tested was suitable for LRP1 immunostaining in rat lung tissue.
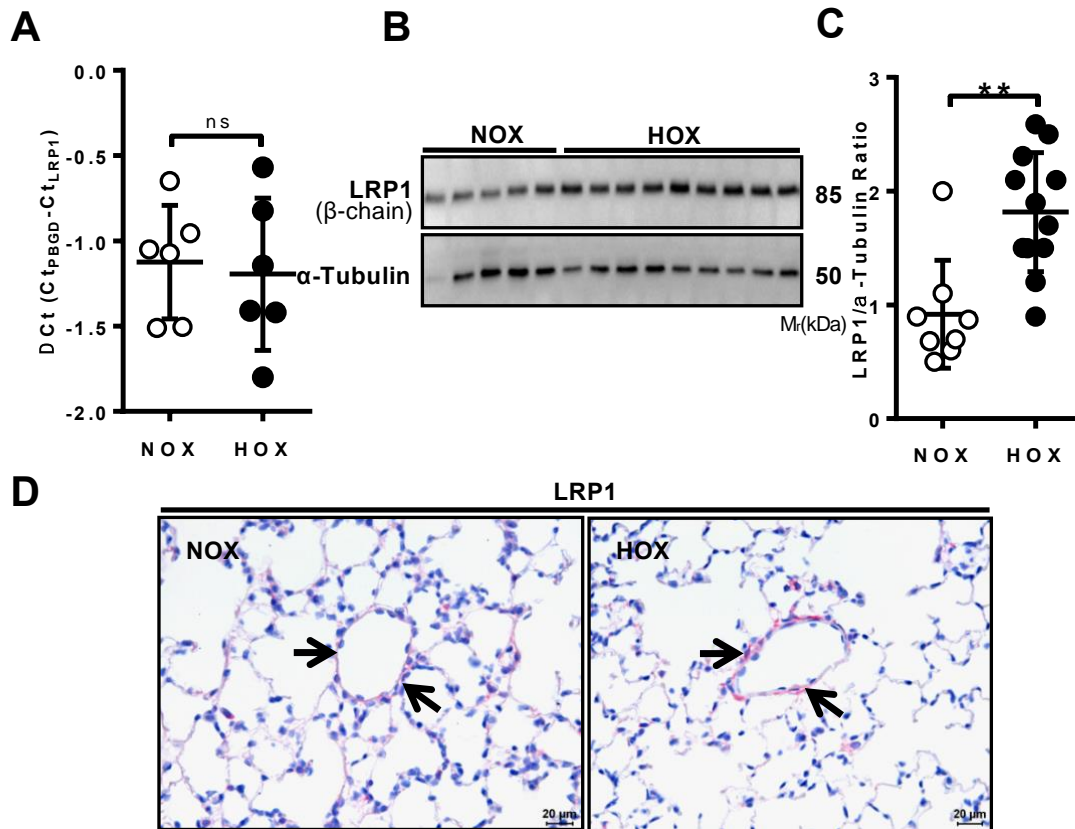
Fig. 4.5 Hypoxia elevates LRP1 protein levels in mouse lungs.

(A, B) LRP1 mRNA (A) and protein levels (B) in lung homogenates of mice maintained either under normoxic (NOX) (n=6 for RNA, n=8 for protein) or hypoxic (HOX) (n=6 for RNA, n=12 for protein) conditions. The qPCR data are expressed as ΔCt using *Pbgd* as a reference gene. For western blotting, α-Tubulin was used as a loading control. Representative blots are shown. (C) Densitometry analysis of (B). (D) Immunohistochemistry for LRP1 in lungs of NOX and HOX mice. Arrows indicate pulmonary vessels. Scale bar = 20 µm. ns, not significant, **p<0.01.

4.3 Regulation of LRP1 expression in PASMC

As PDGF-BB is one of the main mediators of PH, it was interesting to investigate whether this growth factor may influence LRP1 expression in isolated PASMC (26). Treatment of PASMC with PDGF-BB did not elevate LRP1 mRNA levels (Figure 4.6 A). On the protein level, however, a time-dependent increase in the LRP1 expression following exposure of PASMC to PDGF-BB was observed (Figure 4.6 B and 4.6 C).
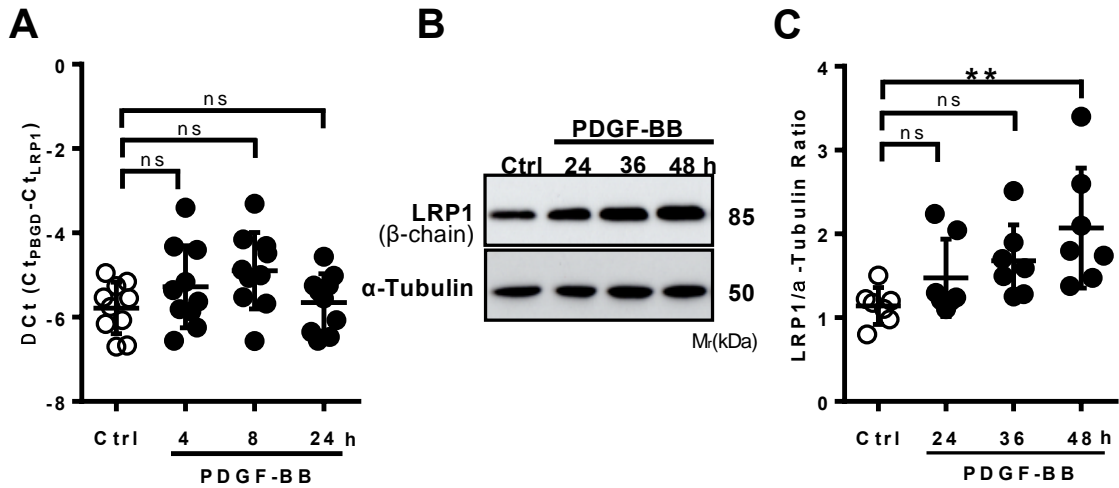
Fig. 4.6 PDGF-BB induces LRP1 protein expression in PASMC.

(A, B) LRP1 mRNA (A) and protein levels (B) in donor PASMC treated with 10 ng/mL of PDGF-BB for indicated time points. The qPCR data are expressed as ΔCt using *PBGD* as a reference gene (n=10). Protein levels were assessed by western blotting using α-Tubulin as a loading control. Representative blots are shown. (C) Densitometry analysis of (B) (n=7). ns, not significant, **p<0.01.

PDGF-BB-induced LRP1 protein expression was attenuated by the PDGF-BB neutralizing antibody or the PDGF receptor antagonist Imatinib (Figure 4.7 A and 4.7 B). Imatinib also attenuated LRP1 synthesis in lung tissue of mice maintained under HOX conditions (Figure 4.7 C and 4.7 D). In addition, LRP1 immunoreactivity was reduced in the pulmonary vessels of HOX mice treated with Imatinib, as compared to controls (Figure 4.7 E).
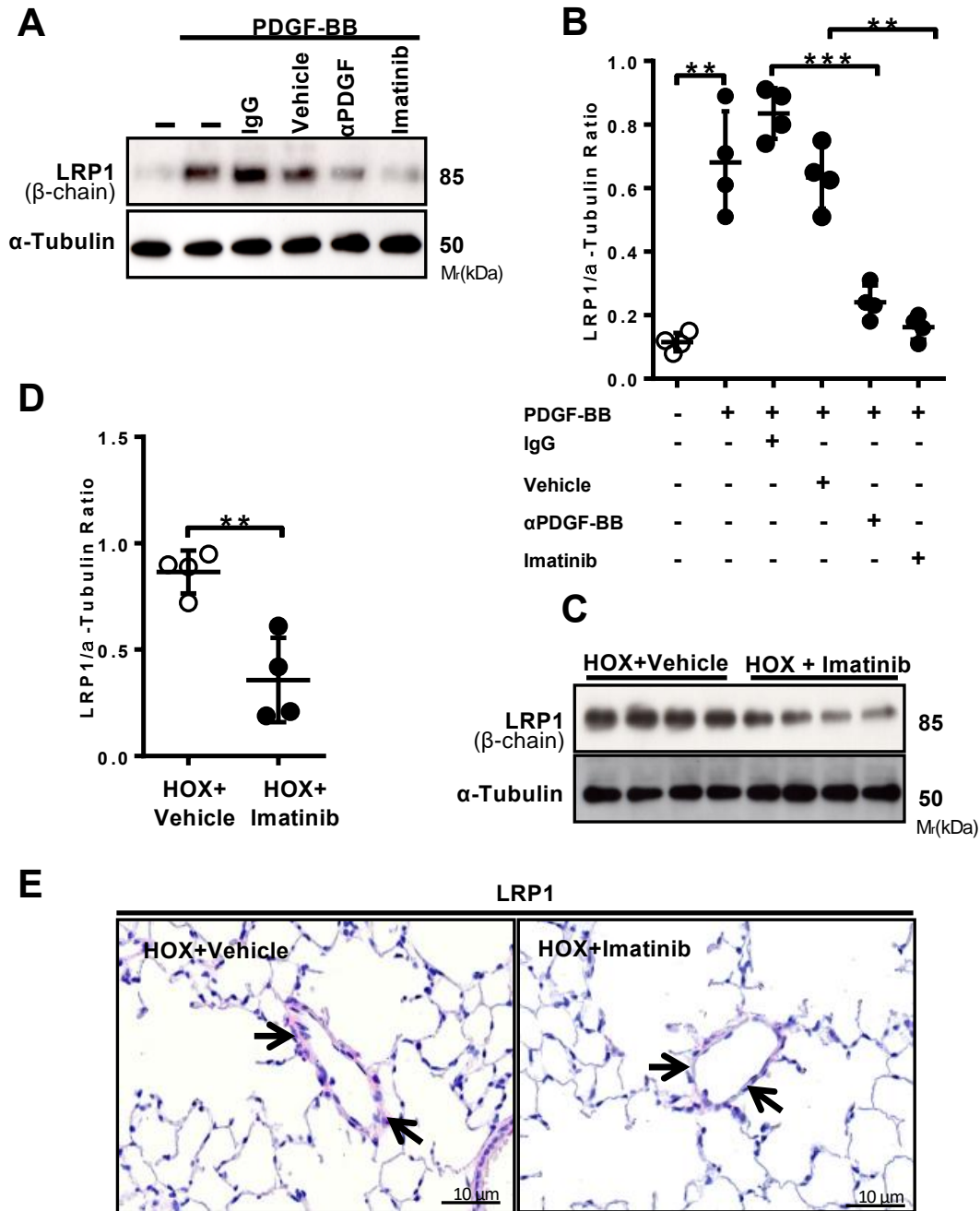
Fig. 4.7 PDGF-BB elevates LRP1 expression in the lungs of mice exposed to hypoxia.

(A) LRP1 protein levels in donor PASMC treated with 10 ng/mL PDGF-BB in the absence or presence of 10 μg/mL of anti-PDGF-BB neutralizing antibody or 2 μM Imatinib. IgG antibody and vehicle were used as controls. For western blotting, α-Tubulin served as a loading control. Representative blots are shown. (B) Densitometry analysis of (A) (n=4). (C) LRP1 protein levels in lung homogenates of mice maintained under hypoxic (HOX) conditions and treated with either vehicle or Imatinib. For western blotting, α-Tubulin served as a loading control. (D) Densitometry analysis of (C) (n=4/group). (E) Immunohistochemistry for LRP1 in lungs of HOX mice treated with either vehicle or Imatinib. Scale bar = 10 μm. ns, not significant, **p<0.01, ***p<0.001.

32

4.4 LRP1 depletion attenuates proliferation of PASMC

Then the impact of LRP1 depletion on PASMC proliferation, adhesion, and migration was analyzed. LRP1 knock-down efficiency is shown in figures 4.8 A and 4.8 B. LRP1 silencing significantly reduced proliferation of PASMC (Figure 4.9 A). On the contrary, migration and adhesion were increased in LRP1 depleted PASMC (Figure 4.9 B-D).
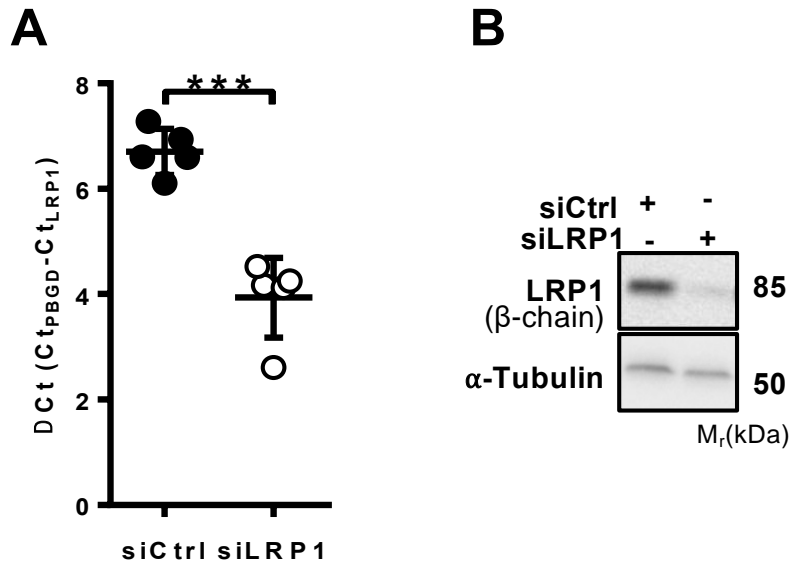
Fig. 4.8 Efficiency of LRP1 knockdown in PASMC.
(A, B) Efficacy of LRP1 knockdown in donor PASMC as assessed by qPCR (A) and by western blotting (B). The qPCR data are expressed as ΔCt using PBGD as a reference gene (n=5). Protein levels were assessed by western blotting using α-Tubulin as a loading control. Representative blots are shown (n=5). ***p<0.001.

In addition, the expression of proteins involved in the PASMC phenotypic switch from a differentiated (contractile) to a de-differentiated (synthetic) state was investigated. The markers of the contractile phenotype are, among others, α-smooth muscle actin (α-SMA) and myocardin (Myoc), whereas the synthetic phenotype is generally characterized by a high expression of ECM components including collagen I (Col I), fibronectin (FN), and osteopontin (OPN) (84).
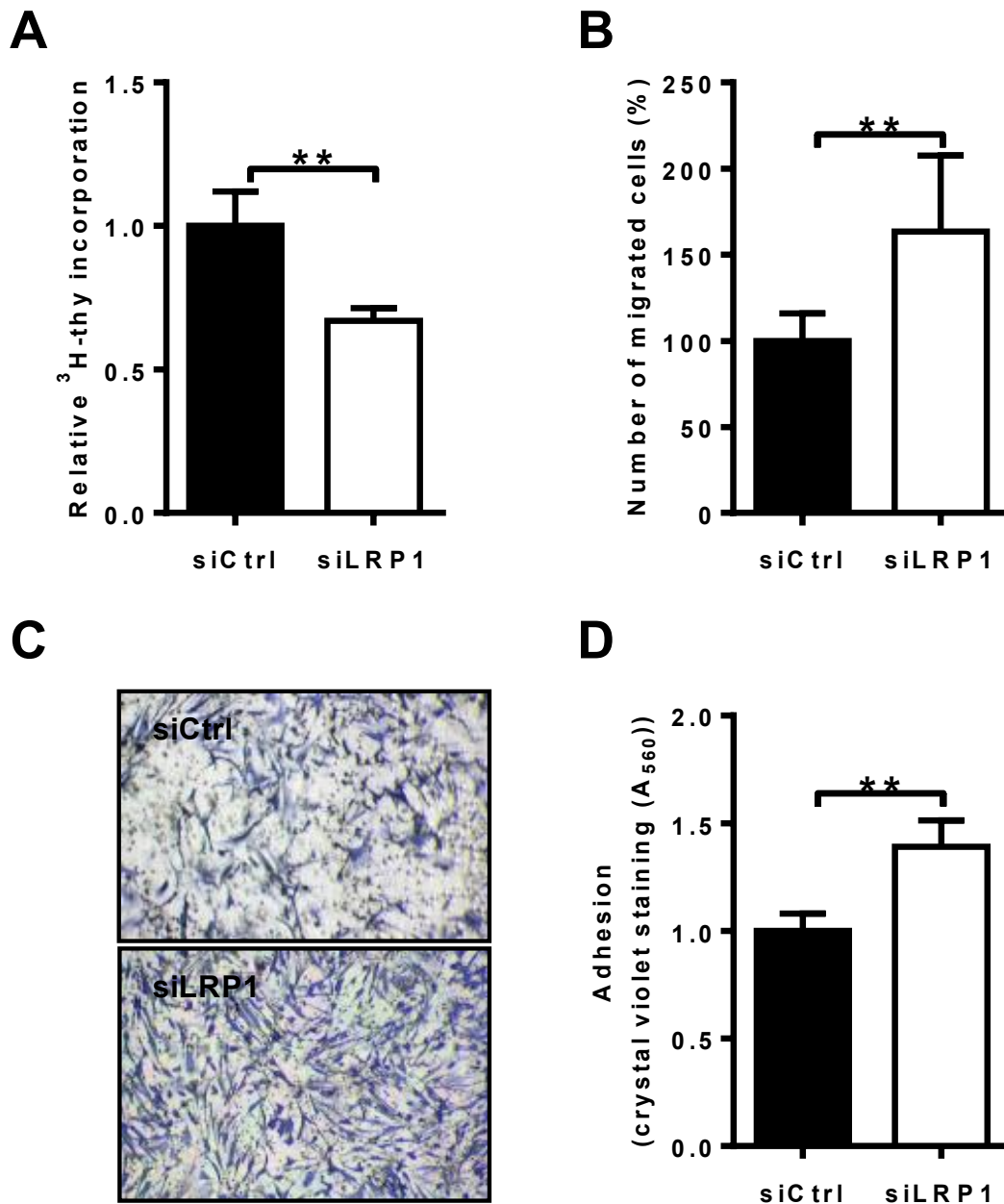
Fig. 4.9 LRP1 depletion reduces PASMC proliferation but increases migration and adhesion of these cells.

(A) Proliferation of donor PASMC treated with either control siRNA (siCtrl) or with siRNA directed against LRP1 (siLRP1) as assessed by ^{3}H-thymidine incorporation (n=4). (B, C) Migration of donor PASMC treated with either siCtrl or siLRP1 as assessed by transwell migration assay. Values were normalized to siCtrl treated cells, which were set to 100% (n=4). Representative images of cells that have migrated through the filter are shown. (D) Adhesion of donor PASMC treated with either siCtrl or siLRP1 to fibronectin as measured by crystal violet staining (n=4). ** p<0.01.

On the mRNA level, the elevation of the Myoc expression following LRP1 silencing was observed (Figure 4.10 A). On the protein level, the changes in the expression of Myoc were accompanied by elevated α-SMA and lower Col I and FN synthesis (Figure 4.10 B

and C). Altogether, these results suggest that low LRP1 levels may support differentiated PASMC phenotype.
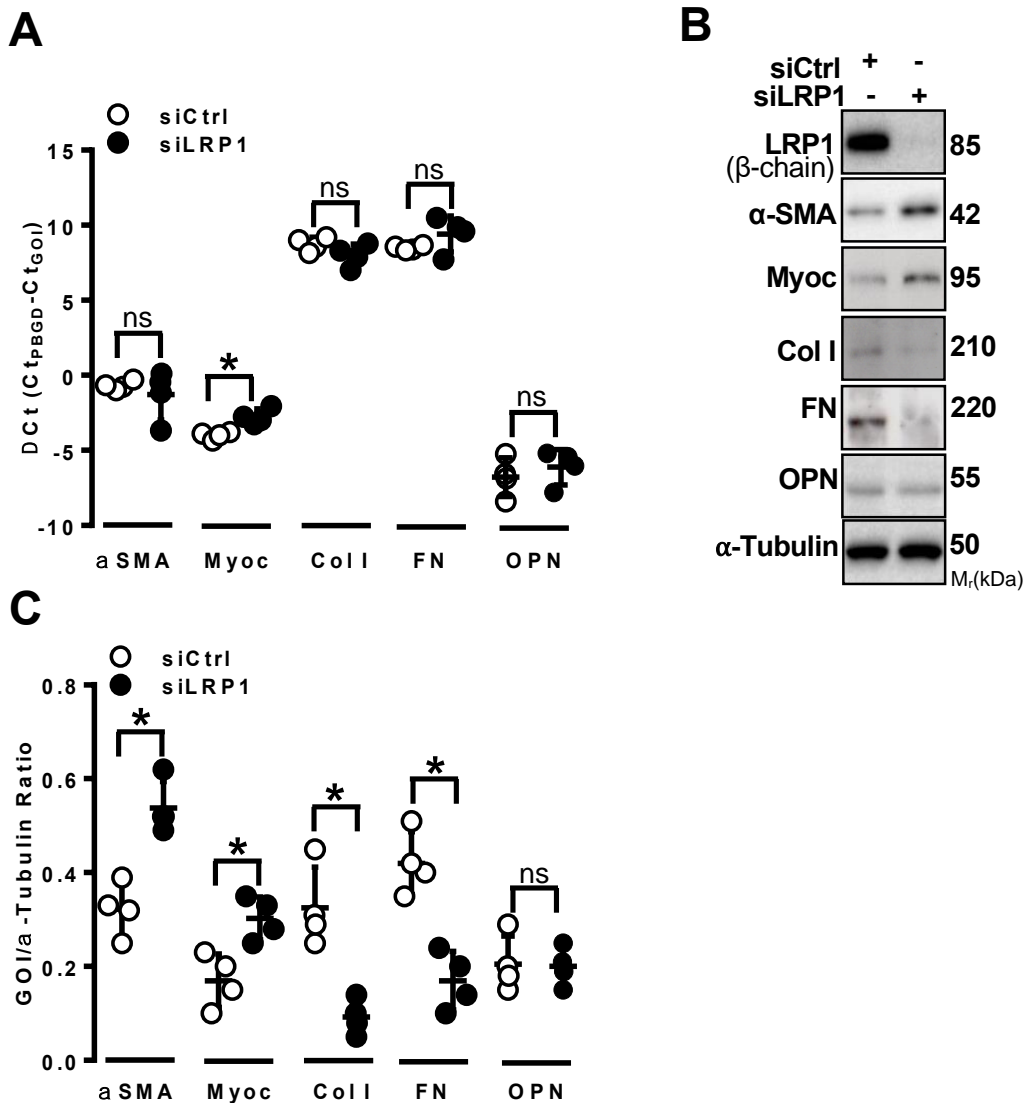
Fig. 4.10 LRP1 knockdown alters PASMC phenotype.

(A, B) mRNA (A) and protein (B) levels of α-smooth muscle actin (α-SMA), myocardin (Myoc), collagen I (Col I), fibronectin (FN), and osteopontin (OPN) in donor PASMC treated with either siCtrl or siLRP1. qPCR results are expressed as ΔCt using *PBGD* as a reference gene (n=4). Protein levels were assessed by western blotting using α-Tubulin as a loading control. (C) Densitometry analysis of (B) (n=4). ns, not significant, *p< 0.05.

4.5 LRP1 regulates proliferation of SMC in 3D *ex vivo* murine lung tissue cultures

To demonstrate that LRP1 controls proliferation of PASMC in more complex biological systems, *Lrp1* gene knock out was performed in precision cut lung slices (PCLS) prepared from Acta2-Cre[ERT2]; Lrp1[flox/flox] mice. As depicted in figures 4.11 A-C the

induction of Cre recombinase activity with 4-hydroxy tamoxifen (4-OH TXN) treatment allowed selective and efficient LRP1 depletion in SMC. Exposure of PCLS generated from Lrp1$^{flox/flox}$ mice to 4-OH TXN excluded the impact of 4-OH TXN on LRP1 expression in pulmonary vessels (Figure 4.11 B and 4.11 C). Trace amounts of LRP1 in 4-OH TXN-treated PCLS derived from Acta2-Cre^{ERT2}; Lrp1$^{flox/flox}$ mice may originate from EC of microdissected pulmonary vessels (Figure 4.11 B and 4.11 C).
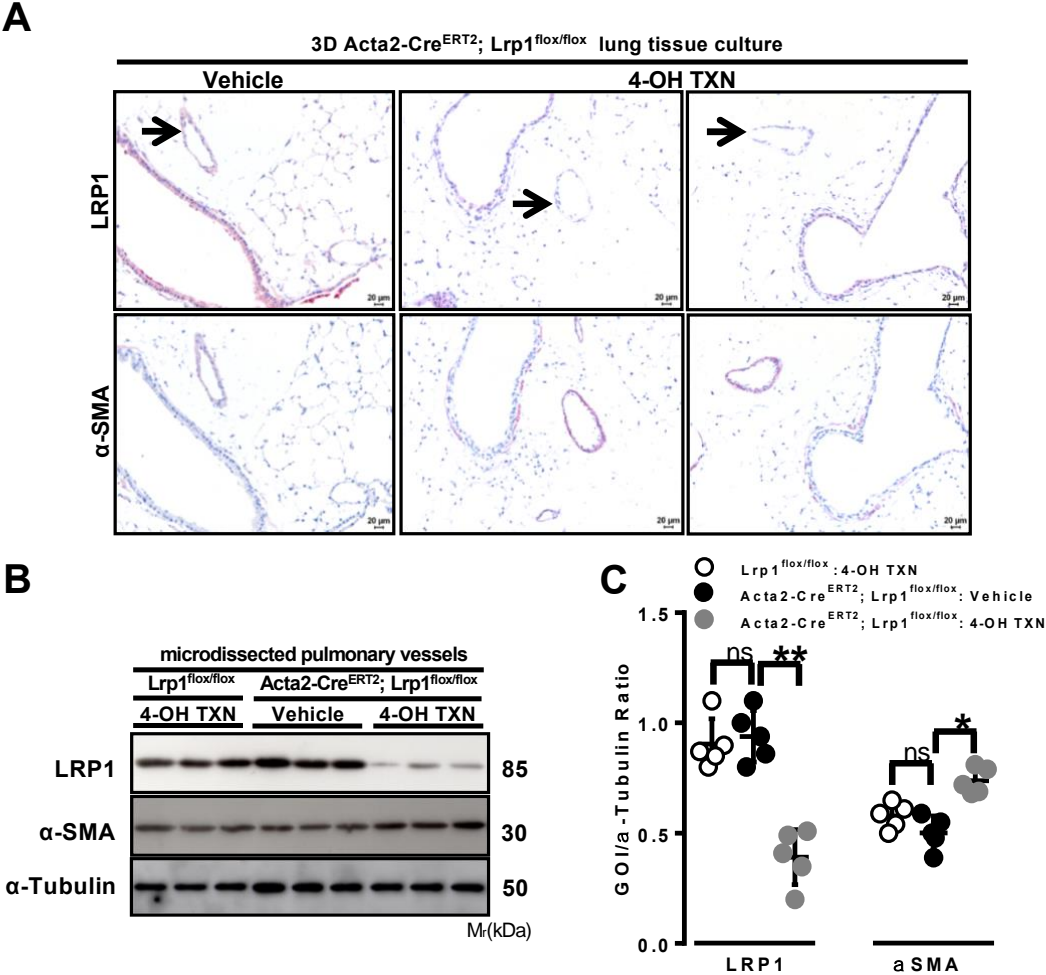
Fig. 4.11 SMC-specific depletion of LRP1 in 3D lung tissue cultures.

(A) Immunoreactivity for LRP1 (upper panel) and α-smooth muscle actin (α-SMA, lower panel) in 3D *ex vivo* Acta2-Cre^{ERT2}; Lrp1$^{flox/flox}$ lung tissue cultures following treatment with vehicle or 4-hydroxy tamoxifen (4-OH TXN). Arrows indicated LRP1 positive and LRP1 negative vessel in vehicle- and 4-OH TXN-treated samples, respectively. Scale bar = 20 μm. (B) LRP1 and α-SMA protein expression in vessels microdissected from 3D *ex vivo* Lrp1$^{flox/flox}$ or Acta2-Cre^{ERT2}; Lrp1$^{flox/flox}$ lung tissue cultures following treatment with vehicle or 4-OH TXN. α-Tubulin served as a loading control in western blotting. Three biological replicates are demonstrated. (C) Densitometry analysis of (B) (n=5). ns, not significant, *p< 0.05, **p<0.01.

Furthermore, 4-OH TXN-induced genetic ablation of *Lrp1* in Acta2-Cre[ERT2]; Lrp1[flox/flox] PCLS increased α-SMA expression in pulmonary vessels (Figure 4.11 B and 4.11 C) and lowered the number of PCNA-positive cells in pulmonary vasculature (Figure 4.12 A and 5 4.12 B).
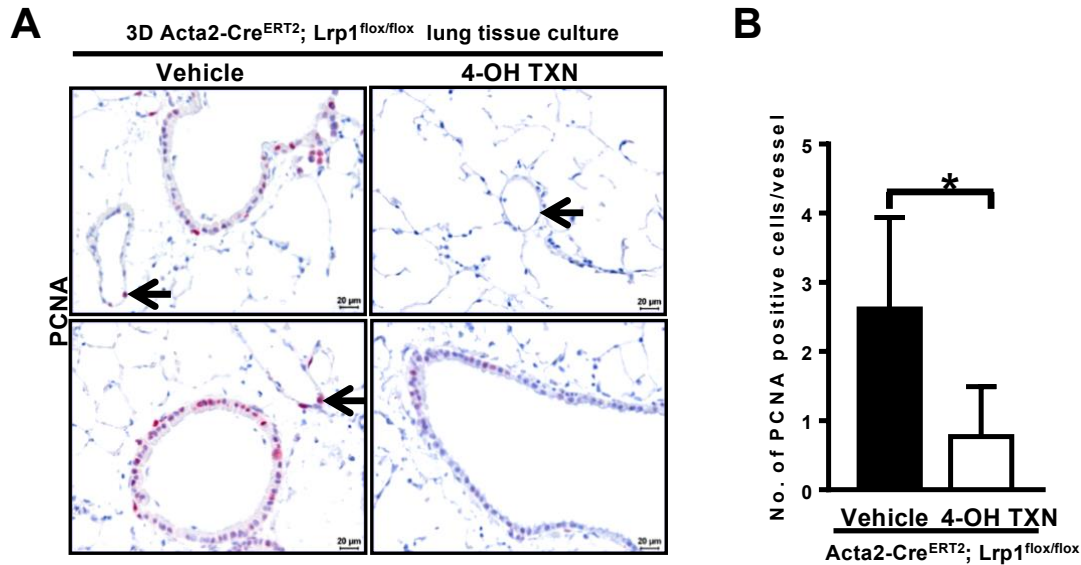
Fig. 4.12 SMC-specific LRP1 knockout decreases proliferation of vascular cells in murine PCLS.
(A) Proliferating cell nuclear antigen (PCNA)-immunostaining in 3D *ex vivo* Acta2-Cre[ERT2]; Lrp1[flox/flox] lung tissue cultures following treatment with vehicle or 4-OH TXN. Arrows indicate PCNA positive cells in pulmonary vessels. Scale bar = 20 µm. (B) Quantification of PCNA- positive cells in 20 pulmonary vessels (20-70 µm diameter) of 4 biological replicates in 3D *ex vivo* Acta2-Cre[ERT2]; Lrp1[flox/flox] lung tissue cultures following treatment with vehicle or 4-OH TXN. ns, not significant, *p< 0.05.

4.6 LRP1 controls cell proliferation *via* regulation of β₁-integrin expression

As cell-ECM interactions are crucial for cell growth and (de)-differentiation, it was interesting to investigate the expression of molecules involved in cell-ECM communication in LRP1- depleted PASMC. LRP1 silencing upregulated mRNA levels of tenascin C (TNC), tissue inhibitor of metalloproteinase (TIMP) 3, MMP8, collagen XV (COL15A1), thrombospondin 2 (THBS2), β₄-integrin (ITGB4) and MMP11. The gene expression levels of matrix metalloproteinase 14 (MMP14), matrix metalloproteinase 13 (MMP13), matrix metalloproteinase 15 (MMP15), α₁-integrin (ITGA1), collagen XI (COL11A1), β₁-integrin (ITGB1) and intercellular adhesion molecule 1 (ICAM1) mRNA were downregulated following LRP1 knockdown (Figure 4.13).
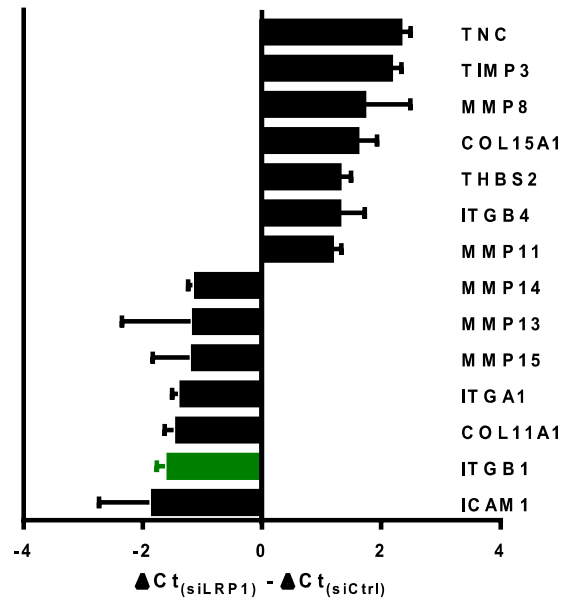
Fig. 4.13 LRP1 depletion regulates expression of molecules involved in extracellular matrix-cell interaction in PASMC.

Genes on extracellular matrix & adhesion molecules RT2 profiler PCR array whose expression was up- or downregulated in donor PASMC by treatment with siRNA directed against LRP1 (siLRP1). The genes listed are those where a statistically significant change (p≤0.05) in relation to mRNA levels observed in mRNA control treated cells was noted. (n=3), *p<0.05.

Integrins are transmembrane receptors that integrate cues from ECM with intracellular signaling machinery, thus regulating multiple cell functions including proliferation (85). Hence, further investigations were focused on the role of integrins in LRP1-triggered changes in PASMC growth. To this end, it was first validated alterations in protein expression of β_1-integrin subunit in PASMC following LRP1 knockdown. As depicted in figures 4.14 A and 4.14 B, silencing of LRP1 reduced the expression of the mature (125 kDa band) and immature (100 kDa band) form of β_1-integrin and lowered the abundance of α_5-integrin (β_1-integrin interaction partner). Likewise, downregulation of β_1- and α_5-integrin expressions were observed in the cytosolic and membrane fraction of LRP1 depleted PASMC (Figure 4.14 C). Concomitantly, the levels of active β_1-integrin on the cell surface of PASMC transfected with LRP1-targetting siRNA were diminished (Figure 4.14 D).
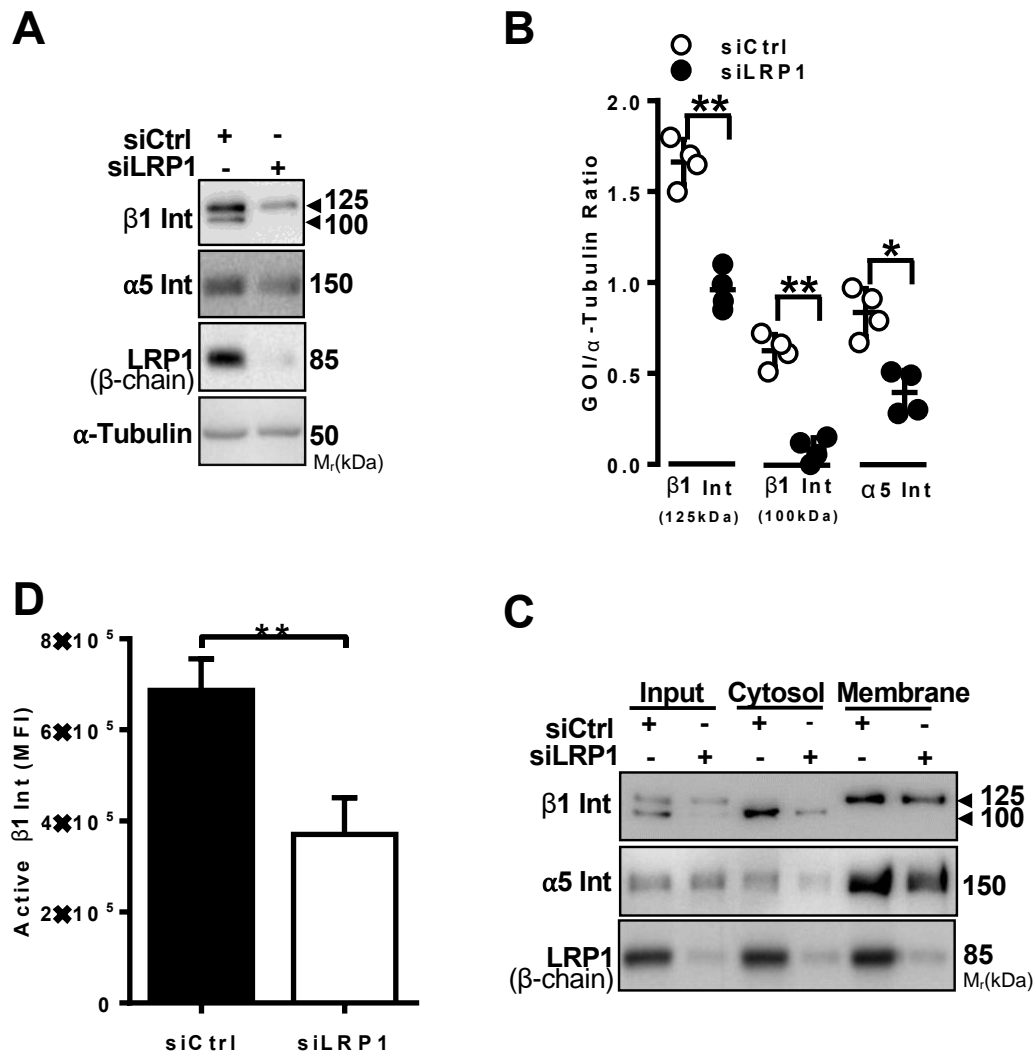
Fig. 4.14 LRP1 reduces the expression and the activity of β₁-integrin in PASMC.
(A) β₁- and α₅- integrin (Int) protein levels in siCtrl- and siLRP1-treated donor PASMC. α-Tubulin served as a loading control in western blotting. Representative blots are shown. (B) Densitometry analysis of (A) (n=4). (C) LRP1, β₁- and α₅- Int protein levels in cytosolic and membrane fractions of siCtrl- or siLRP1-treated donor PASMC. Representative blots are shown (n=3). (D) Active β₁-Int expression levels on cell surface of siCtrl- and siLRP1-treated donor PASMC measured by flow cytometry. The results are expressed as a mean fluorescence intensity (MFI) of active β₁-Int detected with 9EG7 antibody (n=3). *p< 0.05, **p<0.01.

Since reduced proliferation of LRP1-depleted PASMC was accompanied by decreased β₁-integrin levels, it was hypothesized that LRP1 may stimulate PASMC proliferation by supporting β₁-integrin expression. A β₁-integrin function-blocking antibody reduced proliferation of LRP1-expressing PASMC to the level observed in the control cells transfected with LRP1-targeting siRNA (Figure 4.15). Simultaneous LRP1 depletion and β₁-integrin blockage did not further potentiated a growth-inhibitory effect suggesting that LRP1 regulates PASMC proliferation in a β₁-integrin-dependent manner (Figure 4.15).

As LRP1 knockdown altered the expression of β_4-integrin, the functional impact of the increased β_4-integrin levels was also tested in LRP1-depleted PASMC. As seen in figure 4.15, a β_4-integrin blocking antibody did not alter cell proliferation following LRP1 silencing.
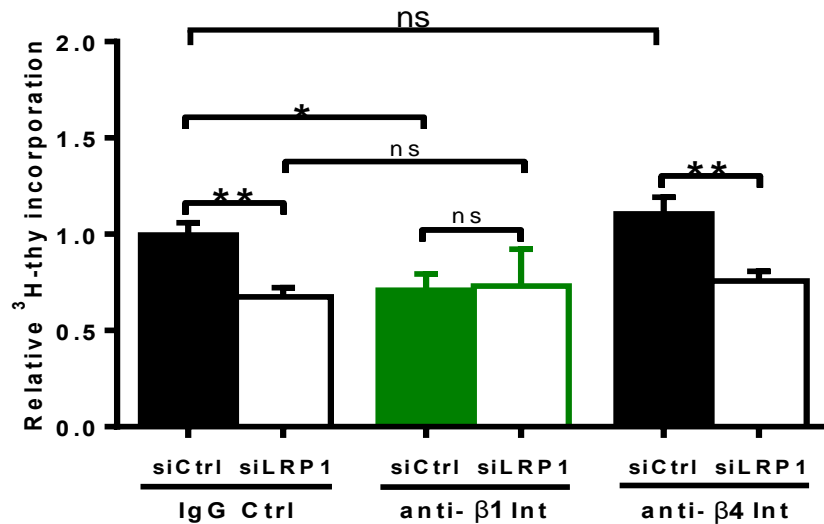
Fig. 4.15 LRP1 regulates proliferation of PASMC in a β_1-integrin-dependent manner.
Proliferation of donor PASMC treated with either siCtrl or siLRP1 in the absence or presence of anti-β_1-Integrin (Int), anti-β_4-Int, or IgG control antibody (IgG Ctrl; 10 µg/mL each) as assessed by ^{3}H-thymidine incorporation (n=5). ns, not significant, *p< 0.05, **p<0.01.

4.7 IPAH PASMC proliferation depends on LRP1-triggered changes in β_1-integrin expression

Next, it was examined whether IPAH PASMC, which exhibit high LRP1 levels, demonstrate elevated expression of β_1-integrin. Indeed, PASMC isolated from IPAH patients displayed significantly increased β_1-integrin expression when compared to the cells isolated from donor lungs (Figure 4.16 A-C). Furthermore, silencing of LRP1 strongly diminished β_1-integrin levels in IPAH PASMC (Figure 4.17 A-B), thus, suggesting a pivotal role of LRP1 in the regulation of β_1-integrin expression under physiological and pathological conditions.
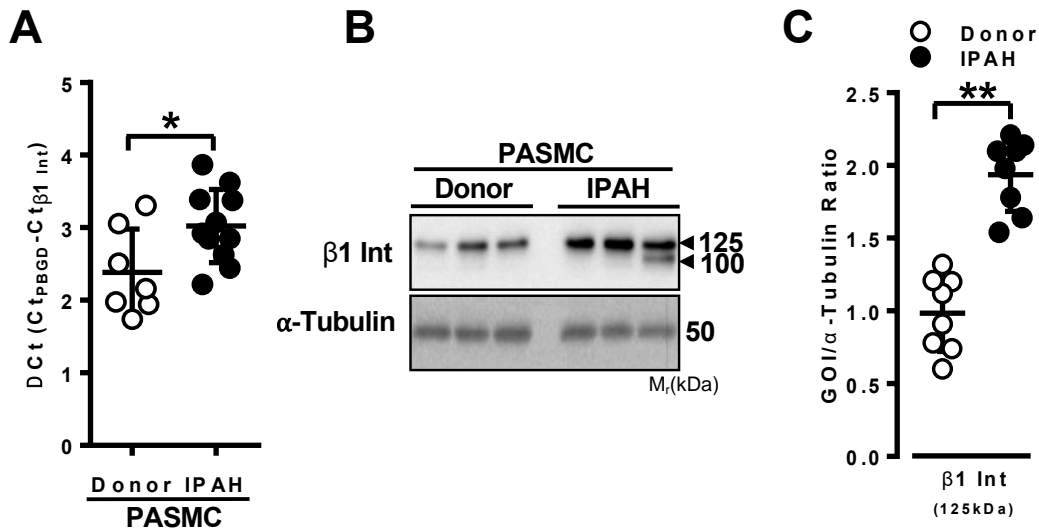
Fig. 4.16 β₁-integrin expression is upregulated in IPAH PASMC.

(A, B) β_1-integrin (Int) mRNA (A) and protein (B) levels in PASMC isolated from of donors (n=7 for RNA) and IPAH patients (n=11 for RNA). The qPCR data are expressed as ΔCt using *PBGD* as a reference gene. For western blotting α-Tubulin was used as a loading control. (C) Densitometry analysis of (B) (n=8). *p<0.05, **p<0.01.

Blockage of β_1-integrin reduced proliferation of IPAH PASMC to the level observed in control donor cells (Figure 4.17 C) and simultaneous LRP1 depletion and β_1-integrin inhibition did not augment the growth-inhibitory effect when compared to IPAH PASMC treated with siLRP1 or the β_1-integrin-blocking antibody alone (Figure 4.17 D). Finally, it was tested whether depletion of LRP1 in PASMC isolated from IPAH lungs may restore their differentiated phenotype. Whereas on the mRNA level the reduction in the expression of OPN following LRP1 silencing was observed (Figure 4.18 A), on the protein level only downregulation of Col I expression in LRP1 depleted samples was apparent (Figure 4.18 B and 4.18 C).
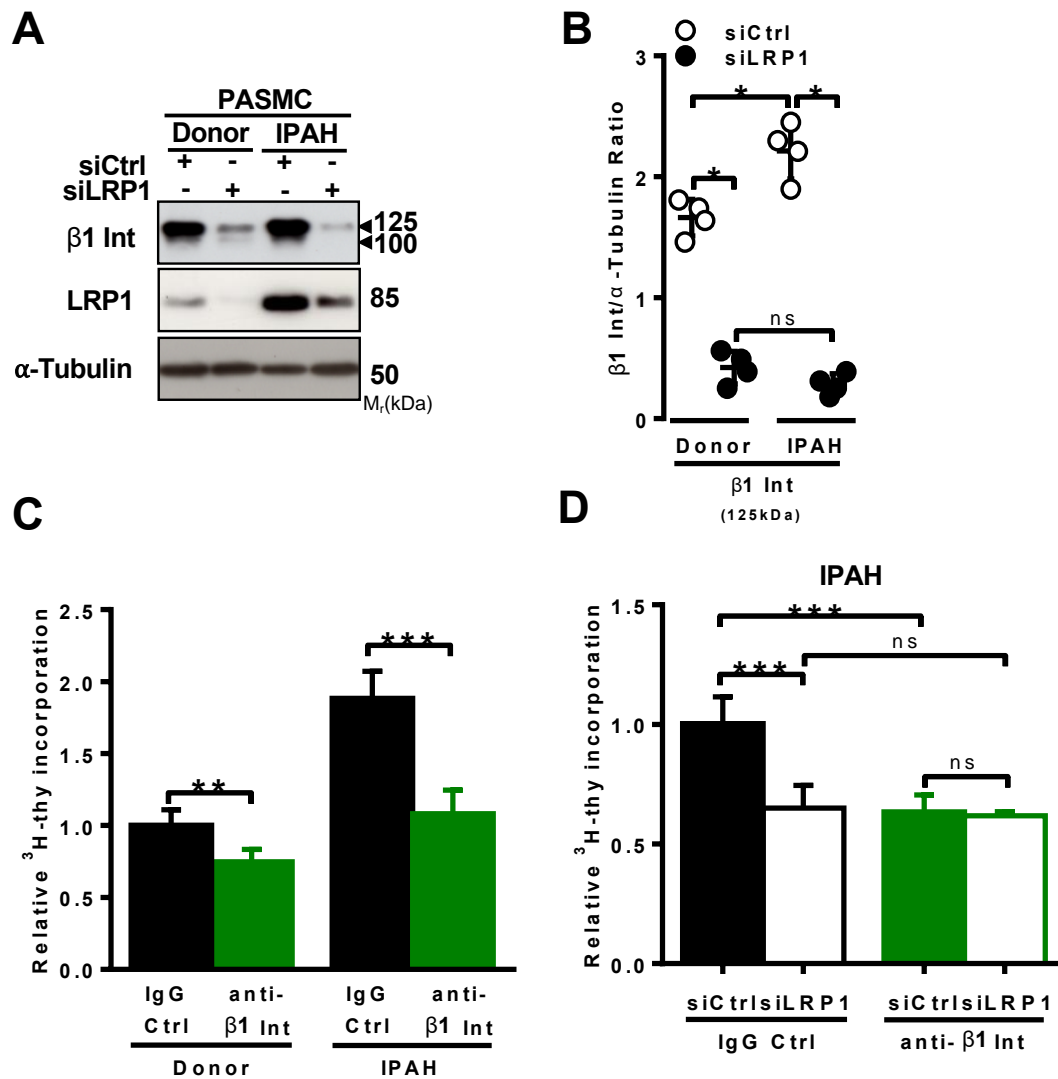
Fig. 4.17 LRP1 orchestrates proliferation of PASMC through β₁-integrin signaling.

(A) β₁-Integrin (Int) protein levels in control siRNA (siCtrl)- and siRNA targeting LRP1 (siLRP1)-treated donor and IPAH PASMC. α-Tubulin was used as a loading control in western blotting. (B) Densitometry analysis of (A) (n=4). (C) Proliferation of donor and IPAH PASMC in the absence or presence of anti-β₁-Int or IgG control antibody (IgG Ctrl; 10 µg/mL each) as assessed by ³H-thymidine incorporation (n=4). (D) Proliferation of IPAH PASMC treated with either siCtrl or siLRP1 in the absence or presence of anti-β₁ Int antibody or IgG Ctrl (10 µg/mL each) as measured by ³H-thymidine incorporation (n=4). *p<0,05, **p<0,01, ***p<0,001; ns, not significant.
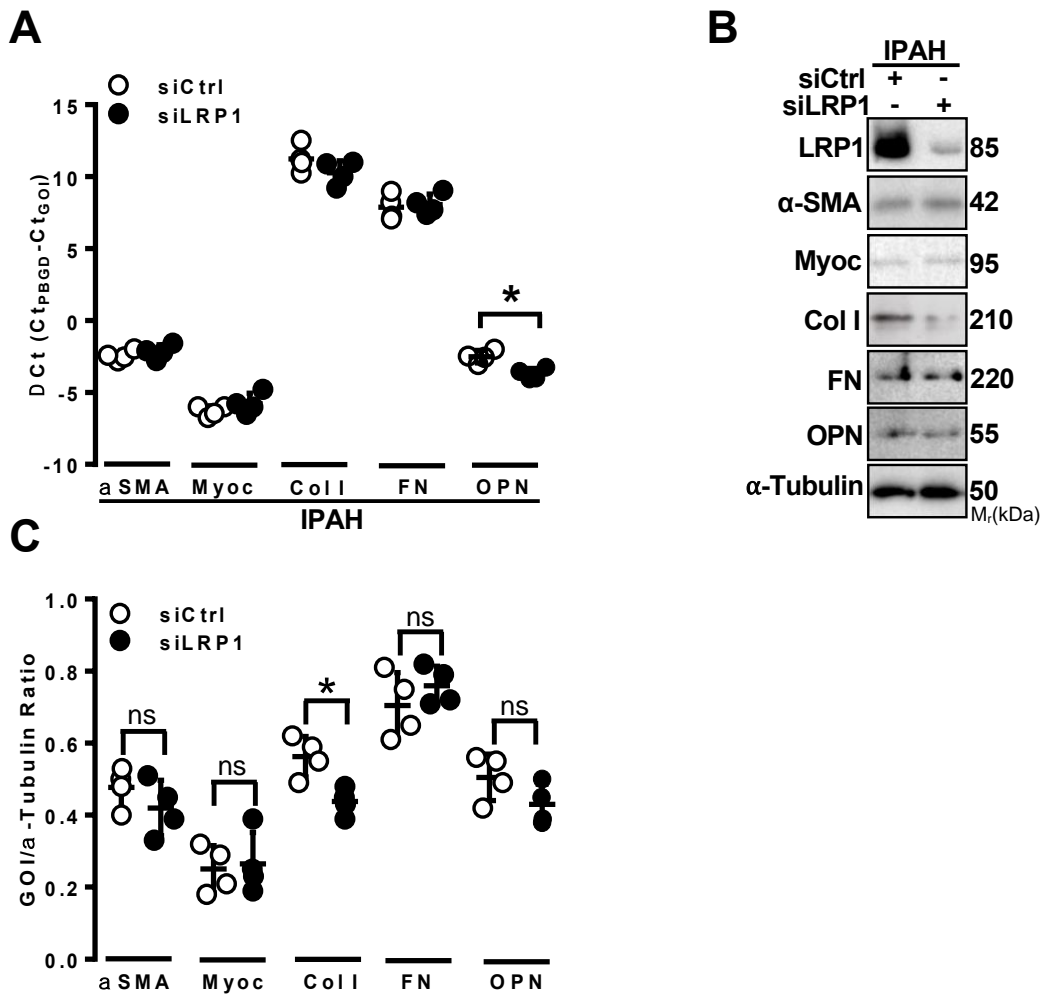
Fig. 4.18 LRP1 does not change expression of phenotype markers in PASMC of IPAH patients.
(A, B) mRNA (A) and protein (B) levels of α-smooth muscle actin (α-SMA), myocardin (Myoc), collagen I (Col I), fibronectin (FN), and osteopontin (OPN) in IPAH PASMC treated with either siCtrl or siLRP1. qPCR results are expressed as ΔCt using *PBGD* as a reference gene (n=4). Protein levels were assessed by western blotting using α-Tubulin as a loading control. (C) Densitometry analysis of (B) (n=4). ns, not significant, *p<0.05.

5. Discussion

5.1 Expression of LRP1 is altered in PASMC and influences their proliferation

The remodeling and occlusion of pulmonary arteries in the context of PAH have not been fully understood yet. Observations such as endothelial dysfunction, PASMC proliferation, and dysregulation of adventitial fibroblasts are the hallmarks of PH. The exact mechanism, however, remains still unclear. Current first line drugs against PAH, PDE5 inhibitors and ET-antagonists lead to the attenuation of experimental PH (86), yet the application of PDE5 inhibitors and ET-antagonists to humans does not cure the disorder. It restores life quality and prolonges survival of these patients. Thus, it is important to further illuminate the pathogenesis of this disorder, in order to find novel therapies.

Here, LRP1 was chosen to be investigated because previous studies have already emphasized the importance of LRP1 in vascular biology. First of all, it was important to verify whether LRP1 expression is changed in diseased pulmonary vessels in contrast to healthy pulmonary vessels. Here in this study, the results show an elevated LRP1 protein expression in the lung tissue and also in PASMC of IPAH patients. Moreover, in two *in vivo* PH models, mice exposed to hypoxia and rats treated with MCT, LRP1 protein expression was also upregulated in the lung tissue. These results might indicate that LRP1 expression changes during the process of remodeling of the pulmonary vessel wall.

LRP1 is not the first member of the LDL receptor family which show an altered expression during the pathogenesis of PH: For example, lectin-like oxidized low density lipoprotein receptor-1 (OLR-1) was reported to be upregulated in hypoxic rats in comparison to their normoxia exposed controls. Isolated PASMC from these rats showed a de-differentiated phenotype following OLR-1 stimulation suggesting that OLR-1 promotes PASMC phenotype switching (87). Another LDL receptor, low density lipoprotein receptor with 11 binding repeats (LR11) was also reported to be involved in the development of PH. Jiang *et al.* reported that LR11 is induced under hypoxic conditions. The inhibition of LR11 in hypoxic mice attenuated right ventricular hypertrophy and vascular thickening of pulmonary arteries. Moreover, higher blood levels of the soluble form of LR11 in PAH patients were found to correlate with a higher mPAP suggesting that soluble LR11 may work as a surrogate parameter for SMC dysfunction in PAH patients (88). Regarding LRP1, little is known about its role in PAH pathogenesis. However, it has been reported that LRP1 is induced in vascular SMC following hypoxia exposure. The mechanism is based on the activation of HIF-1α, which binds to a hypoxia response element in LRP1's promoter region (89). In accordance with the findings that LRP1 is also upregulated in PAH patients and alters PASMC function,

dysregulated LDL receptor expression and function might contribute to the development of PAH.

In contrast to this, in the pathogenesis of atherosclerosis, LRP1 was reported to be essential for SMC function. Depletion of LRP1 in SMC in mice was reported to lead to excessive media proliferation as well as lesions and aneurysm formation of systemic arteries (59). As a conclusion, LRP1 was reported to be crucial in preventing arteriosclerosis. These contrasting findings might be explained by differences between PASMC and systemic SMC. Firstly, PASMC and systemic SMC originate from different embryonic tissues, PASMC are evolving from the pleural mesothelium while systemic SMC derive from the splanchnic mesoderm and the somites (66). Secondly, PASMC and SMC react differently to some environmental changes. For example, whereas hypoxia triggers vasodilation of systemic arteries in order to fulfill the oxygen demand, pulmonary arteries constrict to a hypoxic stimulus in order to guarantee effective oxygenation of blood. One might speculate, that other functions of PASMC and systemic SMC also differ from each other and thus, also selected receptors and signaling cascades work differently in each of them.

Next, it was interesting to study how LRP1 is regulated in PASMC in PH. In vascular smooth muscle cells, HIF-1α was reported to regulate LRP1 expression. Following binding to LRP1's promoter, HIF-1α leads to the elevated mRNA expression of LRP1 (89). In this study, the stimulation of PASMC with PDGF-BB led to an augmented expression of LRP1 with no significant changes on the mRNA level suggesting a mRNA independent regulation. There are many reports in the literature which describe alternative LRP1 regulation, besides mRNA induction. For instance, microRNA (miR) 103/107 is able to inhibit LRP1 expression in PASMC. Deng *et al.* reported that lower levels of miR-103/107 are detected in hypoxia exposed rats and miR-103/107 downregulation in PASMC leads to an aggravated proliferation of these cells (83). There are also reports, that LRP1 can be regulated by its natural antisense transcript (90). Interestingly, in the current study LRP1 elevated expression was neither regulated by mRNA induction nor miR interference. Higher levels of LRP1 were the result of prolonged protein stability, a phenomenon which has previously been reported by Oldonie *et al.* who demonstrated that variants of LRP1 show different protein stability (91). Whether different variants of LRP1 play a role in the pathogenesis of PH, needs to be investigated in future studies. This raises the question what are the consequences for PASMC, if LRP1 activity is augmented in these cells. Low density receptor-related protein 1 has previously been reported to influence proliferation and migration of different cell types including tumor cells. On the one hand, LRP1 promoted invasiveness and reduced adhesion of thyreotic cancer cells while LRP1 depletion in melanoma cells in a xenograft

cancer mice model led to reduced metastasis (92,93). On the other hand, absence of LRP1 led to excessive proliferation of SMC in the aorta of high fat diet mice (61). In this study, LRP1 maintained pro-proliferative effect on PASMC. This result contradicts with previous reports which described that LRP1 decreases proliferation of SMC. However, this might be explained by the fundamental differences between PASMC and arterial SMC.

5.2 Phenotype switching of PASMC is promoted by LRP1

A topic that recently drew much attention is whether SMC experience a phenotype switching in vascular diseases. In the literature, the terms synthetic and contractile are frequently used for the phenotypes of SMC, but this might be misleading since there are many other intermediate phenotypes. Usually, the phenotype is defined by morphology and the expression pattern of several marker proteins. However, the marker proteins of contractile and synthetic PASMC vary throughout the literature. The most common markers of the contractile phenotype are α-SMA and myocardin and the synthetic phenotype, extracellular matrix component proteins such as osteopontin and collagen. Basically, contractile SMC can be observed in full-grown vessels, while synthetic SMC are essential in embryonic vessel formation and are observed in injured vessel walls. Thus, the switching of the phenotype of SMC depends on the environment, which these cells are embedded in. For instance, it was previously reported that an injury of the carotid artery of rats promotes phenotype switching of SMC from a contractile to a synthetic phenotype (94). The phenotype switching was extensively investigated in the context of atherosclerosis, however, in the context of PH this process remains still underexplored. Sahoo *et al.* reported that miR-214 promotes the synthetic phenotype of PASMC in PH (95). Inhibition of miR-214 reduced cell proliferation and increased expression of contractile proteins such as myocardin. Moreover, Lambers *et al.* showed that synthetic PASMC expressed high levels of extracellular matrix components including fibronectin and collagen I (96,97).

LRP1 depletion in donor PASMC increased protein expression of myocardin and α-SMA. Accordingly, LRP1 expressing PASMC had elevated collagen I and fibronectin levels. Interestingly, the expression pattern of these marker proteins was different when it comes to PASMC derived from IPAH patients. The absence of LRP1 in IPAH PASMC neither altered mRNA nor protein levels of myocardin, α-SMA or fibronectin. Only osteopontin mRNA expression and collagen I protein levels were reduced in LRP1 depleted PASMC derived from IPAH patients. In this study, PASMC were isolated from IPAH patients who had underwent lung transplantation. Thus, PASMC from end stage IPAH patients were predominantly used. One might speculate that in other stages of

IPAH, PASMC might show different LRP1 expression with possibly different effects. This speculation is emphasized by the diverse expression pattern of marker proteins when it comes to a LRP1 knockdown in donor PASMC in comparison to IPAH PASMC. Next to contractile and synthetic phenotypes there are also many intermediate phenotypes that were not investigated in this study. It might be the case, that these intermediate phenotypes of PASMC and their characteristics give further critical information and thus, might be crucial to the understanding of the pathogenesis of IPAH. The role of PASMC with an intermediate phenotype requires further investigation in future studies. These results show that donor PASMC may control their phenotype in a LRP1 dependent manner. Contractile protein upregulation and downregulation of extracelluar matrix components suggest that donor PASMC without LRP1 exhibit a contractile phenotype. Thus, LRP1 activity in donor PASMC supports a synthetic phenotype which is observed in developing and pathological arteries. On the other hand, it does not automatically mean that a synthetic phenotype is pathologic. One might speculate, that PASMC respond to the dysfunction of the endothelium and resulting damage by changing their phenotype. This initial, protective response of PASMC may however, get out of control leading to a maintenance and progress of vascular remodeling.

PASMC isolated from IPAH patients do not show phenotype switching in response to LRP1 knockdown, suggesting that LRP1 might be one from many factors involved in the development of pathological alterations of PASMC in PH.

5.3 LRP1 controls PASMC function *ex vivo*

Precision cut lung slices (PCLS) allow the cultivation of lung tissue for several days. This *ex vivo* method permits experiments in a more complex setting and can be also used in testing potential therapeutics in biological systems. Here in this study, PCLS from genetically modified animals were used allowing LRP1 depletion in α-SMA positive cells. PASMC that experienced LRP1 knockout presented less PCNA positive cells in comparison to PASMC expressing LRP1. Conversely, the expression of α-SMA was upregulated in LRP1 depleted PASMC.

At a first glance, a higher expression of α-SMA and low expression of PCNA indicate that LRP1 depleted PASMC possess a differentiated phenotype (98). Notably, lower α-SMA protein expression in murine SMC was associated with vasculopathies such as aortic aneurysm and aortic dissection and these cells were suggested to retain a synthetic phenotype (99). However, α-SMA alone does not precisely define the differentiated status of PASMC. The contractile apparatus is a complex structure containing many proteins that can be separately regulated. Other proteins, that are

relevant to contraction, need to be tested to characterize the phenotype of LRP1 depleted PASMC more precisely in this experimental setting (100).

5.4 LRP1 controls β$_1$-integrin expression in PASMC

Low density lipoprotein receptor-related protein 1 has frequently been described as a key mediator in the regulation of adhesion and de-adhesion. Since adhesion proteins are also important in the process of migration and proliferation, it was interesting to check the impact of LRP1 depletion on these cellular activities in PASMC. Moreover, there are reports that extracellular matrix protein expression pattern changes with the phenotype of arterial SMC, leading to the question whether this also applies to PASMC.

The findings presented in this doctoral work demonstrate that one of the most significantly downregulated genes in LRP1-depleted PASMC was ICAM 1. ICAM 1 is extensively expressed in immature SMC, while its expression is very low in differentiated SMC. One might speculate that ICAM 1 expression is higher in LRP1 expressing PASMC due to the de-differentiated phenotype. In systemic arteries, ICAM 1 is exclusively expressed in a small group of SMC adjacent to neointimal lesions, the role of ICAM 1 in PASMC is however barely described (101, 102). Thus, the changes in ICAM 1 expression are difficult to interpret in this context. Tenascin C (TNC) was highly upregulated in LRP1 knockdown PASMC in comparison to LRP1 expressing PASMC. Tenascin C is an extracellular matrix glycoprotein, that is predominantly expressed during the angiogenesis and in remodeling processes (103). Interestingly, abundant TNC expression in PASMC was observed in rats developing PH and TNC suppression attenuated PH in these animals (104). In the context of the previous results, that LRP1 promotes the synthetic phenotype of PASMC, the upregulation of TNC in LRP1 expressing cells appears to be contradictive. Even though the mRNA of TNC is upregulated in LRP1 depleted PASMC, the protein expression of TNC in these cells might not be enhanced. Thus, further studies are needed to decipher the regulation of TNC protein expression in PASMC.

The changes in mRNA expression of MMP and integrins were the most interesting ones as many MMP and integrin mRNA levels were changed following LRP1 depletion. There are reports, that LRP1 regulates the function of integrins and controls their fate. Previously, Wujak *et al.* described that LRP1 controls degradation of several integrins, including α$_5$-, α$_V$-, β$_1$- and β$_3$-integrin in mouse embryonic fibroblasts. Depletion of LRP1 reduced degradation of these proteins. Moreover, LRP1 was reported to be important for the maturation of β$_1$-integrin and accumulation of unmatured, dysfunctional β$_1$-integrin was observed on the cell surface of LRP1 depleted cells (105).

Here in this study, LRP1 promoted β_1-integrin mRNA expression and resulted in higher β_1-integrin protein expression in PASMC. In contrast to the findings of Wujak *et al.*, LRP1 did not influence the maturation of β_1-integrin in PASMC. Interestingly, an upregulation of $\alpha_5\beta_1$-integrin was described in the synthetic SMC phenotype in association with atherosclerosis and one might speculate, that LRP1 contributes to the process of the phenotype switching by upregulating $\alpha_5\beta_1$-integrin in PASMC. To explore the consequences of β_1-integrin dysregulation in PASMC, it was interesting to investigate the proliferation of these cells. There are conflicting reports whether β_1-integrin promotes or rather inhibits proliferation. For instance, Shibue and Weinberg reported that β_1-integrin promotes proliferation and invasiveness of mouse mammary carcinoma cells (106). On the other hand, β_1-integrin was found to inhibit proliferation in melanoma cells (107). In SMC, β_1- integrin was described to stimulate proliferation and this process could be attenuated by the application of β_1-integrin inhibitory antibody (108). Here in this study, β_1-integrin inhibition reduced proliferation of donor PASMC as well as IPAH PASMC. In order to check whether other integrins are also involved in the process of proliferation, the inhibition of β_4-integrin was tested. β_4-integrin has previously been reported to facilitate proliferation and invasiveness especially in tumor cells (109). Blocking of β_4-integrin did not influence the proliferation of LRP1 knockdown and siRNA control PASMC, suggesting that β_4-integrin is not involved in the process of proliferation of PASMC. In conclusion, proliferation is dictated by LRP1 in a β_1-integrin dependent manner in PASMC isolated from donor and IPAH patients. These results are in accordance with the findings that $\alpha_5\beta_1$-integrin in arterial SMC promotes the synthetic phenotype and thus enhances proliferation (110).

Recently, the involvement of integrins in the pathogenesis of PAH attracted much attention. For instance, OPG, a receptor of the TNFα family, facilitates proliferation in a $\alpha_v\beta_3$-integrin depended manner. OPG was found to aggravate PASMC remodeling and proliferation and its inhibition attenuated the development of PH in a hypoxia-SU5416 mice model. Moreover, a blocking of $\alpha_v\beta_3$-integrin prevented PASMC proliferation. In this study, IPAH PASMC proliferation was increased in comparison to donor PASMC and proliferation of PASMC from IPAH patients and donors could be attenuated by the application of a β_1-integrin inhibitory antibody. Similar to OPG, LRP1 also seems to promote proliferation of PASMC in a β_1-integrin dependent manner. Additionally, integrins regulate vasoconstriction of PASMC by modulating the release of Ca^{2+} from intracellular Ca^{2+} stores (111, 112). In this regard, integrins are pivotal in regulating proliferation, migration and vasocontriction of PASMC. Especially $\alpha_v\beta_3$-integrin was frequently described to promote changes in the proliferation of PASMC and thus to

contribute to vascular remodeling. This study shows that β_1-integrin might also be involved in vascular remodeling in PH.

A recent study by Calvier *et al.* investigated the role of LRP1 in the context of PH in a mouse LRP1 knockout model (113). LRP1 was deleted in SMC (smLRP1$^{-/-}$) leading to the development of spontaneous PH as evident by elevated right ventricular pressure and remodeling of pulmonary arteries. It was previously shown by Boucher *et al.* (59) that LRP1 depletion of systemic SMC deregulates their proliferation and that this effect can be attenuated by a peroxisome proliferator-activated receptor γ (PPARγ) agonist, pioglitazone. The remodeling of pulmonary arteries of smLRP1$^{-/-}$ mice was also attenuated by the application of the PPARγ agonist. Calvier *et al.* concluded that LRP1 depletion deregulates the TGF-β activity consequently leading to the proliferation of PASMC and remodeling of the pulmonary vessels. The authors pointed out that LRP1 is essential for PASMC biology and attenuates the development of PH. On the contrary, this study shows that LRP1 promotes the synthetic phenotype and proliferation of PASMC in a β_1-integrin dependent manner. Although, my results and those reported by Calvier *et* al. seem to be contradictory at a first glance, they both document the pivotal role of LRP1 in the regulation of PASMC activities. Overactivation of LRP1 might lead to phenotype switching and proliferation, while suppression of LRP1 might deregulate TGF-β signaling and thus, promote vascular remodeling and proliferation. It may be that the activity of LRP1 changes from overactivation to suppression and *vice versa* throughout the different stages of PAH resulting in disordered PASMC. Alternatively, the different study design might be responsible for the contradictory results of these studies. Calvier *et al.* used genetically altered mice to induce PH, while this doctoral work focused on human PASMC in *in vitro* and *ex vivo* systems.

Altogether, LRP1 is a scavenger receptor that regulates SMC activities and has already been proven to be relevant in arteriosclerosis, where it plays a crucial role in preserving vascular homeostasis. However, LRP1's role in PASMC is still underreported. This study gives further insights regarding the interaction between LRP1 and the PDGF-BB signaling pathway. Previous reports claimed that LRP1 absence leads to higher expression and phosphorylation of PDGFRβ in a mouse SMC. Here, PDGF-BB induced the expression of LRP1 in mouse PASMC, an event which could represent a negative feedback loop of the PDGF-BB signaling. Considering other reports that link LRP1 and the TGF-β signaling in the development of PH, LRP1 seems to play a central role in controlling TGF-β and PDGF-BB signaling pathways in PASMC.

LRP1 is a multifunctional receptor which integrates many signaling pathway and thus controls plethora of cellular activities. This implies that the expression of LRP1 has to be precisely regulated in the course of the development of PH. Further studies are required

to show whether LRP1 counteracts or rather triggers changes observed in remodeled vessels of IPAH patients.

6. Summary

Pulmonary hypertension (PH) is characterized by thickening of the distal pulmonary arteries caused by media hypertrophy, intima proliferation and vascular fibrosis. In regard to media hypertrophy, phenotype switching of pulmonary artery smooth muscle cells (PASMC) has been frequently observed. This phenotype switch usually occurs in response to injury associated with dysfunction of endothelial cells and leads to conversion of contractile PASMC to synthetic PASMC.

Synthetic PASMC show increased proliferation, migration and expression of extracellular matrix components. Phenotype switching is well described in the context of arteriosclerosis, however, its contribution to the development and progression of PH still remains unexplored. In arteriosclerosis the low density lipoprotein receptor-related protein 1 (LRP1) was described as a scavenger and signaling receptor. By regulating the platelet derived growth factor-BB (PDGF-BB) and the transforming growth factor-β pathways, LRP1 was shown to regulate vascular homeostasis in systemic arteries. Additionally, LRP1 controls recycling and maturation of β_1-integrin and thereby influences proliferation and migration of mouse embryonic fibroblasts. This study examines whether LRP1 controls PASMC activities and thus might contribute to vascular remodeling in PH.

In this study, LRP1 expression was increased in the lungs of idiopathic pulmonary arterial hypertension (IPAH) patients, hypoxia-exposed mice, and monocrotaline- treated rats. PDGF-BB upregulated LRP1 expression in pulmonary artery smooth muscle cells (PASMC). This effect was reversed by the PDGF-BB neutralizing antibody or the PDGF receptor antagonist. Depletion of LRP1 decreased proliferation of donor and IPAH PASMC in a β_1-integrin-dependent manner. Furthermore, LRP1 silencing attenuated the expression of fibronectin and collagen I and increased the levels of α-smooth muscle actin (α-SMA) and myocardin in donor, but not in IPAH, PASMC. In addition, smooth muscle cell-specific LRP1 knockout augmented α-SMA expression in pulmonary vessels and reduced SMC proliferation in 3D *ex vivo* murine lung tissue cultures.

In conclusion, my results indicate that LRP1 promotes dedifferentiation of PASMC and thus contributes to the remodeling of pulmonary vessels in PH. Whether higher LRP1 expression in PASMC from IPAH patients promotes or tries to compensate vascular dysfunction, needs to be answered by future *in vivo* studies.

7. Zusammenfassung

Pulmonale Hypertonie (PH) ist gekennzeichnet durch eine Verdickung von distalen pulmonalen Arterien, welche hervorgerufen wird durch eine Media Hypertrophie, eine Intima Proliferation und durch eine Fibrose der Gefäße. In Bezug auf die Media Hypertrophie zeigte sich, dass die Änderung des Phänotypes von pulmonal arteriellen glatten Muskelzellen (PASMC) häufig beschrieben wurde. Diese Phänotypänderung von PASMC findet üblicherweise statt, wenn Gefäße eine Verletzung oder eine Dysfunktion des Endothels erfahren. Eine Phänotypänderung beschreibt den Wechsel von einem kontraktilen Phänotyp zu einem synthetischen Phänotyp einer glatten Muskelzelle und ist charakterisiert durch erhöhte Proliferation, Migration und erhöhte Ablagerung extrazellulärer Matrixproteine. Dieser Prozess wurde bereits im Zusammenhang mit Arteriosklerose beschrieben. Ob dieser Mechanismus auch relevant sein könnte in der Pathogenese von PH, wurde bisher noch unzureichend erforscht.

„Low density lipoprotein receptor-related protein 1" (LRP1) ist ein Signalrezeptor mit der Fähigkeit zur Endozytose von diversen Liganden und wurde im Zusammenhang mit Arteriosklerose beschrieben. Indem LRP1 Signalwege von „platelet derived growth factor-BB" (PDGF-BB) und "transforming growth factor-β" in systemischen arteriellen SMC reguliert, trägt der Rezeptor so zu einer physiologischen Gefäßfunktion bei. Weiterhin kontrolliert LRP1 den Lebenszyklus sowie die Modifizierung von β_1-Integrin, wodurch Proliferation und Migration reguliert werden in embryonischen Fibroblasten von Mäusen. Diese Arbeit untersucht, ob LRP1 Proliferation, Migration und den Phänotyp von PASMC verändert und ob dies zu einem Remodelling der Gefäße im Kontext von PH beitragen kann.

In dieser Arbeit zeigte sich eine erhöhte LRP1 Protein Expression in den Lungen von Idiopathischer pulmonaler Hypertension (IPAH) Patienten. Dies zeigte sich ebenfalls in Mäusen, welche einer Hypoxie ausgesetzt waren und in Ratten, welche mit Monocrotalin behandelt wurden. Die LRP1 Expression konnte durch PDGF-BB induziert werden. Allerdings konnte dieser Effekt durch PDGF-BB neutralisierte Antikörper bzw. PDGF-BB Antagonisten annulliert werden. PASMC, welche weniger LRP1 exprimiert haben, zeigten eine verminderte Proliferation, welche abhängig von der Expression von β_1-Integrin ist. Weiterhin zeigte eine unterdrückte LRP1 Expression eine verminderte Expression von Kollagen 1, sowie Fibronektin und erhöhte Produktion von „α-smooth muscle actin" (α-SMA). Es zeigte sich zudem eine erhöhte Expression von Myokardin in Donor PASMC, allerdings nicht in IPAH PASMC. Im 3D *ex vivo* Mausmodell, welches aus dünnem Lungengewebe (PCLS) bestand, konnte erfolgreich ein LRP1 Knockout erreicht werden. Unter dem LRP1 Knockout in den PCLS zeigte sich eine verminderte PASMC Proliferation, sowie eine erhöhte Expression von α-SMA.

Schlussfolgernd lässt sich sagen, dass diese Ergebnisse darauf hindeuten, dass LRP1 die Dedifferenzierung, von PASMC begünstigt und dadurch zum Umbau der Lungengefäße im Zusammenhang mit PH beitragen kann. Ob nun eine erhöhte LRP1 Expression in PASMC von IPAH Patientin ein Remodelling der Gefäße unterstützt oder doch kompensiert, muss durch weitere *in vivo* Studien belegt werden.

8. Abbreviations

α-SMA	α-smooth muscle actin
ALK-1	Activin receptor like type 1
ApoE	Apolipoprotein E
ATP	Adenosine triphosphate
BMPR2	Bone morphogenetic protein receptor type 2
BSA	Bovine serum albumin
cAMP	Cyclic adenosine monophosphate
CCB	Ca^{2+} channel blockers
cDNA	Domplementary deoxyribonucleic acid
cGMP	Cyclic guanosine monophosphate
Col I	Collagen I
COL11A1	Collagen XI
COL15A1	Collagen XV
DAPI	4',6-Diamidin-2-phenylindol
dNTP	Nucleoside trisphosphate
ENO-1	Enolase-1
EDTA	Ethylendiamintetraacetat
ET	Endothelin
FBS	Fetal bovine serum
FITC	Fluorescein isothiocyanate
FN	Fibronectin
GMP	Guanosine monophosphate
GOI	Gene of interest
HIF1-α	Hypoxia induced factor-1α
HOX	Hypoxia
ICAM 1	Intercellular adhesion molecule 1
ICD	Intracellular domain
IP3	Phosphatidylinositol-3
IPAH	Idiopathic pulmonary arterial hypertension
ITGA1	Integrin, α_1
ITGB1	Integrin, β_1
ITGB4	Integrin, β_4
kDA	Kilodalton
LDL	Low density lipoprotein
LR11	Low density lipoprotein receptor with 11 binding repeats
LRP1	Low density lipoprotein receptor-related protein 1

MCT	Monocrotaline
MHC	Myosin heavy chain
MMP2	Matrix metalloproteinase 2
MMP8	Matrix metalloproteinase 8
MMP9	Matrix metalloproteinase 9
MMP11	Matrix metalloproteinase 11
mPAP	Mean pulmonary arterial pressure
miRNA	Micro ribonucleic acid
mRNA	Messenger ribonucleic acid
Myoc	Myocardin
NaCl	Sodium chloride
NO	Nitric oxide
NOX	Normoxia
NYHA	New York heart association
OLR-1	Lectin-like oxidized low density lipoprotein receptor-1
OPG	Osteoprotegerin
OPN	Osteopontin
PAEC	Pulmonary arterial endothelial cell
PAH	Pulmonary arterial hypertension
PASMC	Pulmonary arterial smooth muscle cell
PBGD	Porphobilinogen deaminase
PBS	Phosphate buffered saline
PCLS	Precision cut lung slices
PCNA	Proliferating cell nuclear antigen
PDE-5	Phosphodiesterase-5
PDGF	Platelet derived growth factor
PDGFRβ	Platelet derived growth factor receptor β
PGI_2	Prostacyclin
PH	Pulmonary hypertension
PMSF	Phenylmethylsulfonyl fluoride
PPARγ	Peroxisome proliferator-activated receptor γ
PVDF	Polyvinylidene fluoride
qPCR	Quantitative polymerase chain reaction
RHC	Right heart catheterization
RNA	Ribonucleic acid
RPLP0	Ribosomal protein lateral stalk subunit P0
RVSP	Right ventricular systolic pressure

SDS	Sodium dodecyl sulfate
SHP-2	Src homology region 2-containing protein tyrosine phosphatase 2
sLRP1	Soluble low density lipoprotein receptor-related protein 1
siRNA	Small interfering ribonucleic acid
SMC	Smooth muscle cell
SPP1	Osteopontin
SU5416	Semaxanib
TGF-β	Transforming growth factor-β
THBS2	Thrombospondin 2
TIMP3	Tissue inhibitor of metalloproteinase 3
TNC	Tenascin C
TNF-α	Tumor necrosis factor-α
TXN	Tamoxifen
VEGFR	Vascular endothelial growth factor receptor
4-OH TXN	4-hydroxy-tamoxifen
6-MWD	6-minute walking distance

9. List of figures and tables

9.1 List of figures

9.2 List of tables

10. References

1. Galié, N., Humbert, M., Vachiery, JL. *et al.* ECS/ERS Guidelines for the diagnosis and treatment of pulmonary hypertension: The joint task force for the diagnosis and treatment of pulmonary Hypertension of the european society of the cardiology (ESC) and the european respiratory society (ERS): Endorsed by: Association for european paediatric and congenital cardiology (AEPC). *Eur Heart J.* 2016, **37**: 67-119.

2. Hoeper, MM., Ghofrani, A., Grünig, E. *et al.* Pulmonary hypertension. *Dtsch Arztebl Int.* 2017, **130**: 1820-1830.

3. Hoeper, MM., Huscher, D., Ghofrani, HA., *et al.* Elderly patients diagnosed with idiopathic pulmonary arterial hypertension: results from the COMPERA registry. *Int J Cardiol.* 2013, **168**: 871-880.

4. Farber, HW., Miller, DP., Poms, AD. *et al.* Five-year outcomes of patients enrolled in the REVEAL registry. *Chest.* 2015, **148**: 1043-1054.

5. Callan, P. and Clark, AL. Right heart catheterization: Indications and interpretation. *Heart.* 2016, **102**: 147-157.

6. Hoeper, MM., Huscher, D. and Pittrow, D. Incidence and prevalence of pulmonary arterial hypertension in Germany. *Int J Cardiol.* 2016, **203**: 612-613.

7. Wagenvoort, CA., and Wagenvoort, N. Primary pulmonary hypertension: A pathologic study of the lung vessels in 156 clinically diagnosed cases. *Circulation.* 1970, **42**: 1163-1184.

8. Heath, D. and Edwards, JE. The pathology of hypertensive vascular disease: A description of six grades of structural changes in the pulmonary arteries with special reference to congenital cardiac septal defects. *Circulation.* 1958, **18**: 533-547.

9. Tuder., RM., Abman, SH., Braun, T. *et al.* Development and pathology of pulmonary hypertension. *J Am Coll Cardiol.* 2009, **54**: 3-9.

10. Dawson, CA., Grimm, DJ. and Linehan, JH. Influence of hypoxia on the longitudinal distribution of pulmonary vascular resistance. *J Appl Physiol Respir Environ Exerc Physiol.* 1978, **44**: 493-498.

11. Sommer, N., Strielkov, I., Pak, O. *et al.* Oxygen sensing and signal transduction in hypoxic pulmonary vasoconstriction. *Eur Respir J.* 2016, **47**: 288-303.

12. Wolff, HG., Lennox, WG. and Allen, MB. The effect on pial vessels of variations in the oxygen and carbon dioxide content of the blood. *Arch NeurPsych.* 1930, **23**: 1097-1120.

13. Yanagisawa, M., Kurihara, H., Kimura, S. *et al.* A novel potent vasoconstrictor peptide produced by vascular endothelial cells. *Nature.* 1988, **332**: 411-415.

14. Steward, DJ., Levy, RD., Cernacek, P. *et al.* Increased plasma endothelin-1 in pulmonary hypertension: marker or mediator of disease? *Ann Intern Med.* 1991, **114**: 464-469.

15. Giaid, A., Yanagisawa, M., Langleben, D. *et al.* Expression of endothelin-1 in the lungs of patients with pulmonary hypertension. *N Engl J Med.* 1993, **328**: 1732-1739.

16. McCulloch, KM., Docherty, CC., Morecroft, I. *et al.* EndothelinB receptor-mediated contraction in human pulmonary resistance arteries. *Br J Pharmacol.* 1996, **119**: 1125-1130.

17. Biasin, V., Chwalek, K., Wilhelm, J. *et al.* Endothelin-1 driven proliferation of pulmonary arterial smooth muscle cells is c-fos dependent. *Int J Biochem Cell Biol.* 2014, **54**: 137-148.

18. Davenport, AP., Hyndman, KA., Dhaun, N. *et al.* Endothelin. *Pharmacol Rev.* 2016, **68**: 357-418.

19. Tuder, RM., Cool, CD., Geraci, MW. *et al.* Prostacyclin synthase expression is decreased in lungs from patients with severe pulmonary hypertension. *Am J Respir Crit Care Med.* 1998, **159**: 1925-1932.

20. Kuchan, MJ. and Frangos, JA. Role of calcium and calmodulin in flow induced nitric oxide production in endothelial cells. *Am J Physiol.* 1994, **266**: 628-36.

21. Arnold, WP., Mittal, CK., Katsuki, S., *et al.* Nitric oxide activates guanylate cyclase and increases guanosine 3':5'-cyclic monophosphate levels in various tissue preparations. *Proc Natl Acad Sci U S A.* 1997, **74**: 3203-3207.

22. Bogdan, C. Nitric oxide and the immune response. *Nat Immunol.* 2001, **2**: 907-916.

23. Xu, W., Koeck, T., Lara, AR. *et al.* Alterations of cellular bioenergetics in pulmonary artery endothelial cells. *Proc Natl Acad Sci U S A.* 2007, **104**: 1342-1347.

24. Fredriksson, L., Li, H. and Eriksson, U. The PDGF family: four gene products form five dimeric isoform, *Cytokine Growth Factor Rev.* 2004, **15**: 197-204.

25. Demoulin, JB. and Essaghir, A. PDGF receptor signaling networks in normal and cancer cells, *Cytokine Growth Factor Rev.* 2014, **25**: 273-283.

26. Perros, F., Montani D., Dorfmüller, P., *et al.* Platelet-derived Growth factor expression and function in idiopathic pulmonary arterial hypertension, *Am J Respir Crit Care Med.* 2008, **178**: 81-88.

27. Schermuly, RT., Dony, E., Ghofrani, HA. *et al.* Reversal of experimental pulmonary hypertension by PDGF inhibition. *J Clin Invest.* 2005, **115**: 2811-2821.

28. Pankey, EA., Thammasiboon, S., Lasker, GF., *et al.* Imatinib attenuates monocrotaline pulmonary hypertension and has potent vasodilator activity in pulmonary and systemic vascular beds in the rat. *Am J Physiol Heart Circ Physiol.* 2013, **305**: 1288-1296.

29. Vitali, SH., Hansmann, G., Rose, C., *et al.* The Sugen 5416/hypoxia mouse model of pulmonary hypertension revisited: long-term follow-up. *Pulm Circ.* 2014, **4**: 619-629.

30. Ciuclan, L., Hussey, MJ., Burton, V., *et al.* Imatinib attenuates hypoxia-induced pulmonary arterial hypertension pathology *via* reduction in 5-hydroxytryptamine through inhibition of tryptophan hydroxylase 1 expression. *Am J Respir Crit Care Med.* 2013, **187**: 78-89.

31. Frost, AE., Barst, RJ., Hoeper, MM., *et al.* Long-term safety and efficacy of imatinib in pulmonary arterial hypertension. *J Heart Lung Transplant.* 2015, **34**: 1366-1375.

32. Peng, B., Lloyd, P. and Schran, H. Clinical pharmacokinetics of Imatinib. *Clin Pharmacokinet.* 2005, **44**: 879-894.

33. Gatenby, RA. and Gillies, RJ. Why do cancers have high aerobic glycolysis? *Nat Rev Cancer.* 2004, **4**: 891-899.

34. Cottrill, KA. and Chan, SY. Metabolic dysfunction in pulmonary hypertension: The expanding relevance of the Warburg effect. *Eur J Clin Invest.* 2013, **43**: 855-865.

35. Chen, Z., Liu, M., Li, L. *et al.* Involvement of the Warburg effect in non-tumor diseases processes. *J Cell Physiol.* 2018, **233**: 2839-2849.

36. Pfeiffer T., Schuster, S. and Bonhoeffer, S. Cooperation and competition in the evolution of ATP-producing pathways. *Science.* 2001, **292**: 504-507.

37. Archer, SL. Pyruvate kinase and Warburg metabolism in pulmonary arterial hypertension (PAH): uncoupled glycolysis and PAH's cancer-like phenotype. *Circulation.* 2017, **136**: 2486-2490.

38. Bonnet, S., Michelakis, ED., Porter, CJ., *et al.* An abnormal mitochondrial–hypoxia inducible Factor-1α–Kv channel pathway disrupts oxygen sensing and triggers pulmonary arterial hypertension in fawn hooded rats. *Circulation.* 2006, **113**: 2630-2641.

39. Rich, JD. and Rich, S. Clinical Diagnosis of Pulmonary Hypertension. *Circulation.* 2014, **130**: 1820-1830.

40. Badesch, DB., Champion, HC., Sanchez, MA., *et al.* Diagnosis and assessment of pulmonary arterial hypertension. *J Am Coll Cardiol.* 2009, **54**: 55-66.

41. Dabestani, A., Mahan, G., Gardin, JM., *et al.* Evaluation of pulmonary artery pressure and resistance by Pulsed Doppler Echocardiograpy. *Am J Cardiol.* 1987, **59**: 662-668.

42. Augustine, DX., Coates-Bradshaw, LD., Willis, J., *et al.* Echocardiographic assessment of pulmonary hypertension: a guideline protocol from the British Society of Echocardiography. *Echo Res Pract.* 2018, **5**: 11-24.

43. Rosenkranz, S. and Preston, IR., Right heart catheterisation: Best practice and pitfalls in pulmonary hypertension. *Eur Respir Rev.* 2015, **24**: 642-652.

44. Evans, JD., Girerd, B., Montani, D., *et al.* BMPR2 mutations and survival in pulmonary arterial hypertension: an individual participant data meta-analysis. *Lancet Respir Med.* 2016, **4**: 129-137.

45. Trembath, RC., Thomson, JR., Machado, RD., *et al.* Clinical and molecular genetic features of pulmonary hypertension in patients with hereditary hemorrhagic telangiectasia. *N Engl J Med.* 2001, **345**: 325-334.

46. Medarov, BI. And Judson, MA. The role of calcium channel blockers for the treatment of pulmonary arterial hypertension: How much do we actually know and how could they be positioned today? *Respir Med.* 2015, **109**: 557-564.

47. Hu, J., Xu, Q., McTiernan, C., *et al.* Novel targets of drug treatment for pulmonary hypertension. *Am J Cardiovasc Drugs.* 2015, **15**: 225-234.

48. Hernandez-Sanchez, J., Harlow, L., Church, C., *et al.* Clinical trial protocol for TRANSFORM-UK: A therapeutic open-label study of tocilizumab in the treatment of pulmonary arterial hypertension. *Pulm Circ.* 2017, **8**: 1-8.

49. Weinstein, AA., Chin, LM., Keyser, RE. *et al.* Effect of aerobic exercise training on fatigue and physical activity in patients with pulmonary arterial hypertension. *Respir Med.* 2013, **107**: 778- 784.

50. Lund, LH., Khush KK., Cherikh WS., *et al.* The Registry of the International Society for Heart and Lung Transplantation: Thirty-fourth Adult Heart Transplantation Report-2017; Focus Theme: Allograft ischemic time. *J Heart Lung Transplant.* 2017, **36**: 1037-1046.

51. Magruder, JT., Crawford, TC., Grimm, JC., *et al.* Risk factors for de novo malignancy following lung transplantation. *Am J Transplant.* 2017, **17**: 227-238.

52. Herz, J. and Strickland DK. LRP: a multifunctional scavenger and signaling receptor. *J Clin Invest.* 2001, **108**: 779-784.

53. Strickland, DK., Au, DT., Cunfer, P., *et al.* Low-Density lipoprotein receptor–related protein-1 role in the regulation of vascular integrity. *Arterioscler Thromb Vasc Biol.* 2014, **34**: 487-498.

54. May, P., Reddy, YK. and Herz J. Proteolytic processing of low-density lipoprotein receptor-related protein mediates regulated release of its intracellular domain. *J Biol Chem.* 2002, **277**: 18736-18743.

55. Loukinova, E., Ranganathan, S., Kuznetsov, S., *et al.* Platelet-derived growth factor (PDGF)-induced tyrosine phosphorylation of the low-density lipoprotein receptor-related protein (LRP). Evidence for integrated co-receptor function between LRP and the PDGF. *J Biol Chem.* 2002, **277**: 15499-15506.

56. Guttman, M., Betts, GN., Barnes, H., *et al.* Interactions of the NPXY microdomains of the LDL receptor-related protein 1. *Proteomics.* 2009, **9**: 5016-5028.

57. Kui, C. The SHP-2 tyrosine phosphatase: Signaling mechanisms and biological functions. *Cell Res.* 2000, **10**: 279-288.

58. Craig, J., Mikhailenko, I., Noyes, N., *et al.* The LDL receptor-related protein 1 (LRP1) regulates the PDGF signaling pathway by binding the protein phosphatase SHP-2 and modulating SHP-2- mediated PDGF signaling events. *PLoS One.* 2013, **8**: e70432.

59. Boucher, P., Li, WP., Matz, RL., *et al.* LRP1 functions as an atheroprotective integrator of TGFβ and PDGF signals in the vascular wall: Implications for Marfan Syndrome. *PLoS One.* 2007, **2**: e448.

60. Lu, H. and Daugherty, A. Atherosclerosis. *Arterioscler Thromb Vasc Biol.* 2015, **35**: 485-491.

61. Boucher, P., Gotthardt, M., Li, WP., *et al.* Role in vascular wall integrity and protection from atherosclerosis. *Science.* 2003, **300**: 329-332.

62. Overton, CD., Yancey, PG., Major, AS., *et al.* Deletion of Macrophage LDL Receptor– Related Protein Increases Atherogenesis in the Mouse. *Circ Res.* 2007, **100**: 670-677.

63. Llorente-Cortes, V., Royo, T., Juan-Babot, O., *et al.* Adipocyte differentiation-related protein is induced by LRP1-mediated aggregated LDL internalization in human vascular smooth muscle cells and macrophages. *J Lipid Res.* 2007, **48**: 2133-2140.

64. Patel, KM., Strong, A., Tohyama, J., *et al.* Macrophage Sortilin Promotes LDL Uptake, Foam Cell Formation, and Atherosclerosis. *Circ Res.* 2015, **116**: 789-796.

65. Chaabane, C., Coen, M. and Bochaton-Piallat, ML. Smooth muscle cell phenotypic switch: implications for foam cell formation. *Curr Poin Lipidol.* 2014, **25**: 374-379.

66. Wang, G., Jacquet, L., Karamariti, E., *et al.* Origin and differentiation of vascular smooth muscle cells. *J Physiol.* 2015, **593**: 3013-3030.

67. Hamilton, TG., Klinghoffer, RA., Corrin, PD., *et al.* Evolutionary divergence of platelet-derived growth factor alpha receptor signaling mechanisms. *Mol Cell Biol.* 2003, **23**: 4013-4025.

68. Leveen, P., Pekny, M., Gebre-Medhin, S., *et al.* Mice deficient for PDGF B show renal, cardiovascular, and hematological abnormalities. *Genes Dev.* 1994, **8**: 1875-1887.

69. Bonyadi, M., Rusholme, SA., Cousins, FM., *et al.* Mapping of a major genetic modifier of embryonic lethality in TGFβ1 knockout mice. *Nat Genet.* 1997, **15**: 207-211.

70. Allahverdian, S., Chaabane, C., Boukais, K., *et al.* Smooth muscle cell fate and plasticity in atherosclerosis. *Cardiovasc Res.* 2018, **114**: 540-550.

71. Rensen, SS., Doevendans, PA. and van Eys, GJ. Regulation and characteristics of vascular smooth muscle cell phenotypic diversity. *Neth heart J.* 2007, **15**: 100-108.

72. Rzucidlo, EM., Martin, KA. and Powell, RJ. Regulation of vascular smooth muscle cell differentiation. *J Vasc Surg.* 2007, **45**: 25-32.

73. Stiebellehner, L., Frid, MG., Reeves, JT., *et al.* Bovine distal pulmonary arterial media is composed of a uniform population of well-differentiated smooth muscle cells with low proliferative capabilities. *Am J Physiol Lung Cell Mol Physiol.* 2003, **285**: 819-828.

74. Losa, M., Latorre, V., Andrabi, M., *et al.* A tissue-specific, Gata6-driven transcriptional program instructs remodeling of the mature arterial tree. *Elife.* 2017, **6**: 31362.

75. Orr, AW., Hastings, NE., Blackman, BR., *et al.* Complex regulation and function of the inflammatory smooth muscle cell phenotype in atherosclerosis. *J Vasc Res.* 2014, **47**: 168-180.

76. Dai, J., Zhou, Q., Chen, J., *et al.* Alpha-enolase regulates the malignant phenotype of pulmonary artery smooth muscle cells *via* the AMPK-Akt pathway. *Nat Commun.* 2018, **9**: 3850.

77. Umesh, A., Paudel, O., Cao, YN., *et al.* Alteration of pulmonary artery integrin levels in chronic hypoxia and monocrotaline-induced pulmonary hypertension. *J Vasc Res.* 2011, **48**: 525-537.

78. Jia, D., Zhu, Q., Liu, H., *et al.* Osteoprotegerin disruption attenuates HySu-induced pulmonary hypertension through integrin αvβ3/FAK/AKT pathway suppression. *Circ Cardiovasc Genet.* 2017, **10**: e001591.

79. Gairhe, S., Bauer, NN., Gebb, SA., *et al.* Myoendothelial gap junctional signaling induces differentiation of pulmonary arterial smooth muscle cells. *Am J Physio Lung Cell Mol Physiol.* 2011, **301**: 527-535.

80. Guo, H., Liu, W., Ju Z., *et al.* An efficient procedure for protein extraction from formalin-fixed, paraffin-embedded tissues for reverse phase protein arrays. *Proteome Sci.* 2012, **10**: 56.

81. Wendling, O., Bornert, JM., Chambon, P., *et al.* Efficient temporally-controlled targeted mutagenesis in smooth muscle cells of the adult mouse. *Genesis.* 2009, **47**: 8-14.

82. Rohlmann, A., Gotthardt, M., Willnow, TE., *et al.* Sustained somatic gene inactivation by viral transfer of Cre recombinase. *Nat Biotechnol.* 1996, **14**: 1562-1565.

83. Deng, B., Du, J., Hu, R., *et al.* MicroRNA-103/107 is involved in hypoxia-induced proliferation of pulmonary arterial smooth muscle cells by targeting HIF-1β. *Life Sci.* 2016, **147**: 117-124.

84. Wanjare, M., Kuo, F. and Gerecht, S. Derivation and maturation of synthetic and contractile vascular smooth muscle cells from human pluripotent stem cells. *Cardiovasc Res.* 2013, **97**: 321-330.

85. Moreno-Layseca, P. and Streuli, CH. Signalling pathways linking integrins with cell cycle progression. *Matrix Biol.* 2014, **34**: 144-153.

86. Cavasin, MA., Demos-Davies, KM., Schuetze, KB., *et al.* Reversal of severe angioproliferative pulmonary arterial hypertension and right ventricular hypertrophy by combined phosphodiesterase-5 and endothelin receptor inhibition. *J Transl Med.* 2014, **12**: 314.

87. Zhang, W., Zhu, T., Wu, W., *et al.* LOX-1 mediated phenotypic switching of pulmonary arterial smooth muscle cells contributes to hypoxic pulmonary hypertension. *Eur J Pharmacol.* 2018, **818**: 84-95.

88. Jiang L., Konishi, H., Nurwidya, F., *et al.* Deletion of LR11 attenuates hypoxia-induced pulmonary arterial smooth muscle cell proliferation with medial thickening in mice. *Arterioscler Thromb Vasc Biol.* 2016, **36**: 1972-1979.

89. Castellano, J., Aledo, R., Sendra, J., *et al.* Hypoxia stimulates low-density lipoprotein receptor–related protein-1 expression through hypoxia-inducible factor-1α in human vascular smooth muscle mells. *Arterioscler Thromb Vasc Biol.* 2011, **31**: 1411-1420.

90. Yamanaka, Y., Faghihi, MA., Magistri, M., *et al.* Antisense RNA controls LRP1 sense transcript expression through interaction with a chromatin-associated protein. *Cell Rep.* 2015, **11**: 967-976.

91. Oldoni, F., van Capelleveen, JC., Dalilia, N., *et al.* Naturally occurring variants in LRP1 (Low-Density Lipoprotein Receptor–Related Protein 1) affect HDL (High-Density Lipoprotein) metabolism through ABCA1 (ATP-Binding Cassette A1) and SR-B1 (Scavenger Receptor Class B Type 1) in humans. *Arterioscler Thromb Vasc Biol.* 2018, **38**: 1440-1453.

92. Langloit, B., Perrot, G., Schneider, C., *et al.* LRP-1 promotes cancer cell invasion by supporting ERK and inhibiting JNK signaling pathways. *PLoS One.* 2010 **5**: e11584.

93. Montel, V., Gaultier, A., Lester RD., *et al.* The low-density lipoprotein receptor–related protein regulates cancer cell survival and metastasis development. *Cancer Res.* 2007, **67**: 9817-9824.

94. Mano, T., Luo, Z., Malendowicz, SL, *et al.* Reversal of GATA-6 downregulation promotes smooth muscle differentiation and inhibits intimal hyperplasia in balloon-injured rat carotid artery. *Circ Res.*1999, **84**: 647-654.

95. Sahoo S., Meijles DN., Al Ghouleh, I., *et al.* MEF2C-MYOCD and Leiomodin1 suppression by miRNA-214 promotes smooth muscle cell phenotype switching in pulmonary arterial hypertension. *PLoS One.* 2016, **11**: e0153780.

96. Lambers C., Roth, M., Zhong, J., *et al.* The interaction of endothelin-1 and TGF-β1 mediates vascular cell remodeling. *PLoS One.* 2013, **8**: e73399.

97. Saker, M., Lipskaia, L., Marocs, E., *et al.* Osteopontin, a key mediator expressed by senescent pulmonary vascular cells in pulmonary hypertension. *Arterioscler Thromb Vasc Biol.* 2016, **36**: 1879-1890.

98. Campbell, JH., Kocher, O., Skalli, O., *et al.* Cytodifferentiation and expression of alpha-smooth muscle actin mRNA and protein during primary culture of aortic smooth muscle cells. Correlation with cell densitiy and proliferative state. *Arteriosclerosis.* 1989, **9**: 633-643.

99. Yuan, SM. and Wu, N. Aortic α-smooth-muscle actin expressions in aortic disorders and coronary artery disease: An Immunohistochemical study. *Anatol J Cardiol.* 2018, **19**: 11-16.

100. Gomez, D. and Owens, GK. Smooth muscle cell phenotypic switching in atherosclerosis. *Cardiovasc Res.* 2012, **95**: 156-164.

101. Printseva O., Peclo, MM. and Tjurmin, AV., A 90-k-Da surface antigen of immature smooth muscle cells is ICAM-1. *Am J Physiol.* 1991, **261**: 21-22.

102. Braun M., Pietsch, P., Schroer, K., *et al.* Cellular adhesion molecules on vascular smooth muscle cells. *Cardiovasc Res.* 1999, **41**: 395-401.

103. Imanaka-Yoshida, K., Yoshida, T. and Miyagawa-Tomita, S. Tenascin-C in development and disease of blood vessels. *Anat Rec (Hoboken).* 2014, **297**: 1747-1757.

104. Cowan, KN., Jones, PL. and Rabinovitch, M. Regression of hypertrophied rat pulmonary arteries in organ culture is associated with suppression of proteolytic activity, inhibition of Tenascin-C, and smooth muscle cell apoptosis. *Circ Res.* 1999, **84**: 1223-1233.

105. Wujak, L., Boettcher RT., Pak, O., *et al.* Low-density lipoprotein receptor-related protein 1 couples β1 integrin activation to degradation. *Cell Mol Life Sci.* 2018, **75**: 1671-1685.

106. Shibue, T. and Weinberg, RA. Integrin β1-focal adhesion kinase signaling directs the proliferation of metastatic cancer cells disseminated in the lungs. *Proc Natl Acad Sci U S A.* 2009, **106**: 10290-10295.

107. Ritsma L., Dey-Guha, I., Talele, N., *et al.* Integrin β_1 activation induces an anti-melanoma host response. *PLoS One.* 2017, **12**: e0175300.

108. Ichii, T., Koyama, H., Tanaka, S., *et al.* Thrombospondin-1 mediates smooth muscle cell proliferation induced by interaction with human platelets. *Arterioscler Thromb Vasc Biol.* 2002, **22**: 1286-1292.

109. Bertotti, A., Comoglio, PM and Trusolino L. β_4 Integrin is a transforming molecule that unleashes met tyrosine kinase tumorigenesis. *Cancer Res.* 2005, **65**: 10674-10679.

110. Finney, AC, Stokes KY., Pattilo CB., *et al.* Integrin signaling in atherosclerosis. *Cell Mol Life Sci.* 2017, **74**: 2263-2282.

111. Umesh, A., Thompson, MA, Chini, EN. *et al.* Integrin ligands mobilize Ca2+ from ryanodine receptor-gated stores and lysosome-related acidic organelles in pulmonary arterial smooth muscle cells. *J Biol Chem.* 2006, **281**: 34312-34323.

112. Welschoff, J., Matthey, M. and Wenzel, D. RGD peptides induce relaxation of pulmonary arteries and airways *via* β_3-integrins. *FASEB J.* 2017, **28**: 2281-2292.

113. Calvier, L., Boucher, P., Herz, J., *et al.* LRP1. Deficiency in vascular SMC leads to pulmonary arterial hypertension that is reversed by PPARγ. *Circ Res.* 2019, **124**: 1778-1785.

11. Acknowledgments

First of all, I would like to thank my supervisor Prof. Dr. Malgorzata Wygrecka-Markart. I am grateful for the chance to work in your research group. Your guidance, patients, and excellent advices paved the way for this doctoral work. I could not have asked for a better supervisor and I am very proud to say that I was a part of your research group.

Moreover, I would like to thank my PostDoc Dr. Lukasz Wujak for being an exemplary teacher. Your unlimited support, motivation and guidance, rouse my interest in science.

I would like to express my gratitude to Dr. Dariusz Zakrzewicz and Dr. Miroslava Didiasova for having on open ear and being supportive every day. It was a pleasure to work with you in the lab.

I am very grateful to all lab members especially Yvonne, Horst, Markus and Simone.

I would also like to thank Aleksander Petrovic, Grazyna Kwapiszewska, Ralph Schermuly, Anna Gungl, Walter Klepetko and Liliana Schäfer.

I am grateful for all the support and love I experienced from my family, Markus, Claudia and Verena, throughout this challenging time. Coming home was a relief after an intense week of studying and researching. Last but not least, I am blessed having a wonderful partner, Alina, who has encouraged me every single day.

12. Declaration

„Hiermit erkläre ich, dass ich die vorliegende Arbeit selbständig und ohne unzulässige Hilfe oder Benutzung anderer als der angegebenen Hilfsmittel angefertigt habe. Alle Textstellen, die wörtlich oder sinngemäß aus veröffentlichten oder nichtveröffentlichten Schriften entnommen sind, und alle Angaben, die auf mündlichen Auskünften beruhen, sind als solche kenntlich gemacht. Bei den von mir durchgeführten und in der Dissertation erwähnten Untersuchungen habe ich die Grundsätze guter wissenschaftlicher Praxis, wie sie in der „Satzung der Justus-Liebig-Universität Gießen zur Sicherung guter wissenschaftlicher Praxis" niedergelegt sind, eingehalten sowie ethische, datenschutzrechtliche und tierschutzrechtliche Grundsätze befolgt. Ich versichere, dass Dritte von mir weder unmittelbar noch mittelbar geldwerte Leistungen für Arbeiten erhalten haben, die im Zusammenhang mit dem Inhalt der vorgelegten Dissertation stehen, und dass die vorgelegte Arbeit weder im Inland noch im Ausland in gleicher oder ähnlicher Form einer anderen Prüfungsbehörde zum Zweck einer Promotion oder eines anderen Prüfungsverfahrens vorgelegt wurde. Alles aus anderen Quellen und von anderen Personen übernommene Material, das in der Arbeit verwendet wurde oder auf das direkt Bezug genommen wird, wurde als solches kenntlich gemacht. Insbesondere wurden alle Personen genannt, die direkt und indirekt an der Entstehung der vorliegenden Arbeit beteiligt waren. Mit der Überprüfung meiner Arbeit durch eine Plagiatserkennungssoftware bzw. ein internetbasiertes Softwareprogramm erkläre ich mich einverstanden."

_____   _____

Ort/ Datum   Unterschrift